Stratigraphy and dating of a lake sediment record from Lyngsjön, eastern Scania—human impact and aeolian sand deposition during the last millennium

Marijana Stevic

Dissertations in Geology at Lund University,
Master's thesis, no 555
(45 hp/ECTS credits)

Department of Geology
Lund University
2019

Stratigraphy and dating of a lake sediment record from Lyngsjön, eastern Scania—human impact and aeolian sand deposition during the last millennium

Master's thesis

Marijana Stevic

Department of Geology
Lund University

2019

Contents

Cover Picture: Lake Lyngsjön, north-eastern Scania. Photo: Marijana Stevic

Abstract

MARIJANA STEVIC

Stevic, M., 2019: Stratigraphy and dating of a lake sediment record from Lyngsjön, eastern Scania—human impact and aeolian sand deposition during the last millennium. *Dissertations in Geology at Lund University*, No. 555, 33 pp. 45 hp (45 ECTS credits).

Abstract: A small lake in north-eastern Scania, southern Sweden, Lake Lyngsjön, reveals a long history of aeolian sand drift based on a 3 meter long sediment sequence covering the last approximately 1400 years. Human impact, primarily through intensified land use and decreased forest cover, has periodically led to increased aeolian sand drift both locally and regionally. Elevated C/N ratios suggest a period of increased forest cover close to the lake as seen primarily through elevated pine pollen frequencies during the 10^{th} century and later during the 18^{th} century. Agricultural changes such as the 19^{th} century land amalgamation, which would have led to enhanced wind erosion of fields, was simultaneously countered through the plantation of trees, which hampered transportation of aeolian sand into the lake. The continuation of intensified agricultural activity after the implementation of land amalgamation successively led to increased deposition of aeolian sand during the onset of the 20^{th} century. Organic and carbonate contents of the sediments are generally anti-correlated for the majority of the succession although changes in land use during the past 100 years, with substantial input of aeolian sand around the 1920s, seem to have had a major impact on the total inorganic carbon (TIC) signal; possibly by a reduction in carbonate producing algae. Later agricultural changes during the 1940s did not have any major effects on the lake since the plantation of pine and spruce in proximity of the lake acted as a shelter for aeolian sand drift. Correlations between the reconstructed aeolian sand content within the more recent part of the succession and documented historical events have been used to explain earlier aeolian sand deposition events during the 10^{th} and 12^{th} century. A continuous record of cultivated pollen points towards an uninterrupted human influence having an effect on the lake sediments during the past millennium. Maps from the 17^{th} century and onwards reveal a close relationship between past aeolian sand deposition and changes in forest extent on a local to regional scale.

Keywords: aeolian activity, aeolian sand deposition, human impact, geochemistry, lake sediments, land use, pollen

Supervisors: Dan Hammarlund, Karl Ljung

Subject: Quaternary Geology

Marijana Stevic, Department of Geology, Lund University, Sölvegatan 12, SE-223 62 Lund, Sweden. E-mail: stevicmar@gmail.com

Svensk sammanfattning

MARIJANA STEVIC

Stevic, M., 2019: Stratigraphy and dating of a lake sediment record from Lyngsjön, eastern Scania—human impact and aeolian sand deposition during the last millennium. *Examensarbeten i geologi vid Lunds universitet*, Nr. 555, 33 sid. 45 hp.

Sammanfattning: En liten sjö, Lyngsjön, i nordöstra Skåne, södra Sverige, avslöjar en lång historia av eolisk aktivitet baserat på en 3 meter lång sedimentsekvens som omfattar de senaste 1400 åren. Mänsklig inverkan, främst genom intensifierad markanvändning och minskad utbredning av skog, har lett till ökad eolisk sand drift både lokalt och regionalt. En ökning i C/N förhållanden tyder på en period med ökad utbredning av skog i närheten av sjön som även kan ses genom en ökning i tallpollenförekomster under 900-talet samt senare under 1700-talet. Jordbruksförändringar så som 1800-talets landändringsreformer som borde ha inneburit en ökning i vinderosion av jordbruksmarker, motverkades istället av en samtida plantering av träd vilket hindrade transporten av eolisk sand till sjön. Den fortsatta påtagliga jordbruksverksamheten efter sammanslagningen av jordbruksenheter (s.k. enskiftet) ledde successivt till ökad deposition av eolisk sand i början av 1900-talet. Mängden organiskt material samt mängden karbonater i sedimenten visar på en generell anti-korrelation genom majoriteten av sedimentsuccessionen, dock inte under de senaste 100 åren då en betydande mängd sand avsattes under 1920-talet vilket verkar ha påverkat den totala mängden oorganiskt kol; möjligtvis genom en minskning av karbonatproducerande alger. Jordbruksförändringar under 1940-talet och framåt verkar inte ha haft en stor inverkan på sjön. Detta främst i samband med att det planterades träd (tall och gran) i närheten av sjön vilket fungerade som ett skydd mot inkommande eolisk sand till sjön. Jämförelser mellan rekonstruerad mängd eolisk sand för de mer recenta delarna av successionen och dokumenterade historiska händelser, användes för att kunna förklara tidigare deposition av eolisk sand under 900-talet samt 1100-talet. En kontinuerlig förekomst av pollen från odlade växter tyder på en oavbruten påverkan av sjösedimenten till följd av mänsklig aktivitet under det senaste milleniet. Kartor från 1600-talet framåt visar på en nära koppling mellan historisk deposition av eolisk sand och ändringar i utbredning av skog både lokalt och regionalt.

Nyckelord: eolisk aktivitet, eolisk sand deposition, mänsklig inverkan, geokemi, sjösediment, markanvändning, pollen

Handledare: Dan Hammarlund, Karl Ljung

Ämnesinriktning: Kvartärgeologi

Marijana Stevic, Geologiska institutionen, Lunds Universitet, Sölvegatan 12, 223 62 Lund, Sverige. E-post: stevicmar@gmail.com

1 Introduction

Wind erosion, a process involving the depletion of soils with the removal of sand and silt and often organic matter, has been a topic of several studies since it became a national concern in the 1940s (Bärring et al. 2003). Examples with significant impact can be seen in southern and eastern Scania where several coherent agricultural fields have been left either covered by thick layers of sand or left barren consisting of only coarse grained material (Åhman 1974; Mattson et al. 1978, 1983; Lidmar-Bergström et al. 1983; Bärring et al. 2003).

This trend in increased wind erosion during the last century has been favoured by human impact, primarily through structural changes in agriculture, which demanded the removal of hedges, tree fences and stone walls around arable fields acting as protection against the wind drift (Åhman 1974; Bärring et al. 2003). A similar situation with the degradation of soils and increased sand drift in Scania has previously been observed by Carl von Linné and Anders Tidström in the mid-1700s (Linné 1751; Weibull 1891), indicating that sand drift has been a recurrent problem in Scania.

The importance of a vegetation cover to counteract soil erosion by immobilizing sand and silt has been discussed by several authors (e.g. Åhman 1974; Bärring et al. 2003; Li et al. 2004; Breshears et al. 2009; Ravi et al. 2010). Wind erosion has proven to be most severe during the spring due to the absence of vegetation and drier soil conditions (Åhman 1974; Mattsson et al. 1978). Areas with glacifluvial deposits such as the Kristianstad Plain contain abundant sand in the soils (Agrell 1980, 1981; Lidmar-Bergström et al. 1983), which is released and transported as aeolian sand as a consequence of decreasing vegetation through human impact (Li et al. 2004).

The sand fraction most prone to erosion as analysed at two sites on the Vomb Plain (south-central Scania) reveals approximately 60-70% medium sand (0.2-0.6 mm) (Åhman 1974). The presence of larger quantities of aeolian sand grains larger than 0.2 mm on bogs in Halland, south-western Sweden, have further been interpreted as a result of an opening of the landscape due to human impact through intensified land use; as indicated by pollen (de Jong et al. 2006, 2007). Land use history as investigated by pollen analysis of lake sediments in the Ystad area (southern Scania) reveal approximately 3000 years of human impact connected to agricultural activities leading to increased soil erosion near the lakes (Gaillard & Berglund 1988; Gaillard et al. 1991a, 1991b).

Increased soil erosion coupled with land use changes through human impact has been further inferred from studying the geochemistry of lake sediments (e.g. Meyers 2003; Köster et al. 2005; Enters et al. 2006, 2008; Li et al. 2008; Bragée et al. 2013). Studies of geochemical records reveal two principle sources of organic matter (terrestrial and algal) deposited in lake sediments (Meyers & Lallier-Vergès 1999; Meyers & Teranes 2001). Elevated C/N ratios (approx. 16 and higher) of lake sediments point towards elevated input of terrestrial organic matter, which can be seen in lakes having been affected by humans e.g. through deforestation (Kaushal & Binford 1999; Wolfe et al. 1999). A mixed contribution of algal and terrestrial organic matter to lake sediments usually provide C/N ratios between 13-14 (Meyers & Teranes 2001). Lakes affected by late 19th century industrial waste (high N contribution) generally display lower C/N ratios in their sediments, and in combination with higher total organic carbon (TOC) point towards algal productivity (C/N ratios $\leq$ 10) as the main contributor of organic matter (Meyers 2003; Routh et al. 2004). Total inorganic carbon (TIC), used to identify carbonates derived from e.g. soils (Enters et al. 2010), or in-lake production through algal activity (Hammarlund et al. 2005), can be further diluted by input of minerogenic material through increased aeolian activity and catchment erosion (Enters et al. 2010).

To be able to recognize human impact contributions to sand drift, sand accumulation rates and geochemical records obtained from a lake sediment sequence from Lake Lyngsjön (Fig. 1A and B) have been analysed and compared with a pollen record from the same sample succession. These data are used to describe the sand drift history during the last 1400 years on the Kristianstad Plain where this process has been a reoccurring problem for the local population.

This thesis has been conducted as part of a collaboration between the National Historical Museums, the Swedish National Heritage Board and the Department of Geology, Lund University. The Bachelor thesis of Björn Olsenius (Olsenius 2014), where historical sand drift on the Kristianstad Plain was investigated, has been used as a basis for a more detailed reconstruction of sand drift as recorded from the lake sediments.

The aim of this thesis is to establish a chronology for the Lake Lyngsjön sediment record and to quantify past changes in medium sand deposition aided by geochemical and lithostratigraphic data. The reconstructed aeolian sand deposition is used to evaluate past aeolian sand drift on the Kristianstad Plain as a result of human impact as indicated by historical documents and previous studies in the area. The specific method used to reconstruct past aeolian sand drift and its potential limitations are discussed.

1.1 Study area and site description

Lake Lyngsjön is situated on the Kristianstad Plain (north-eastern Scania), approximately 15 km south-southwest of Kristianstad (Fig. 1A). The Lyngsjö village and church are situated within 500 m northeast of the lake. The lake, with a maximum depth of 6 m, is relatively small, approx. 250 x 300 m and is dewatered through a narrow trench north of the lake into the Vramsån River (Fig. 1B and C) (Friman & Hyll 2015; County Administrative Board of Scania 2016). The surface of the lake is situated at 20 m a.s.l. The local bedrock consists of sandstones and limestones (60 m thick at Lake Lyngsjön) deposited on the gneiss-dominated basement during the younger Cretaceous (ca. 75 Ma years ago) (Lagerås 2004; Regnéll 1980).

The calcareous strata at Lake Lyngsjön are covered by Quaternary deposits consisting of carbonate-rich till superimposed by glacifluvial sand with a thickness of 10-30 m (Regnéll 1980). The lake is characterized as a dead-ice lake and its recharge is primarily supplied as carbonate-rich groundwater (Regnéll 1980; County Administrative Board of Scania 2016). The lake was once connected with a small lake named Älvasjön

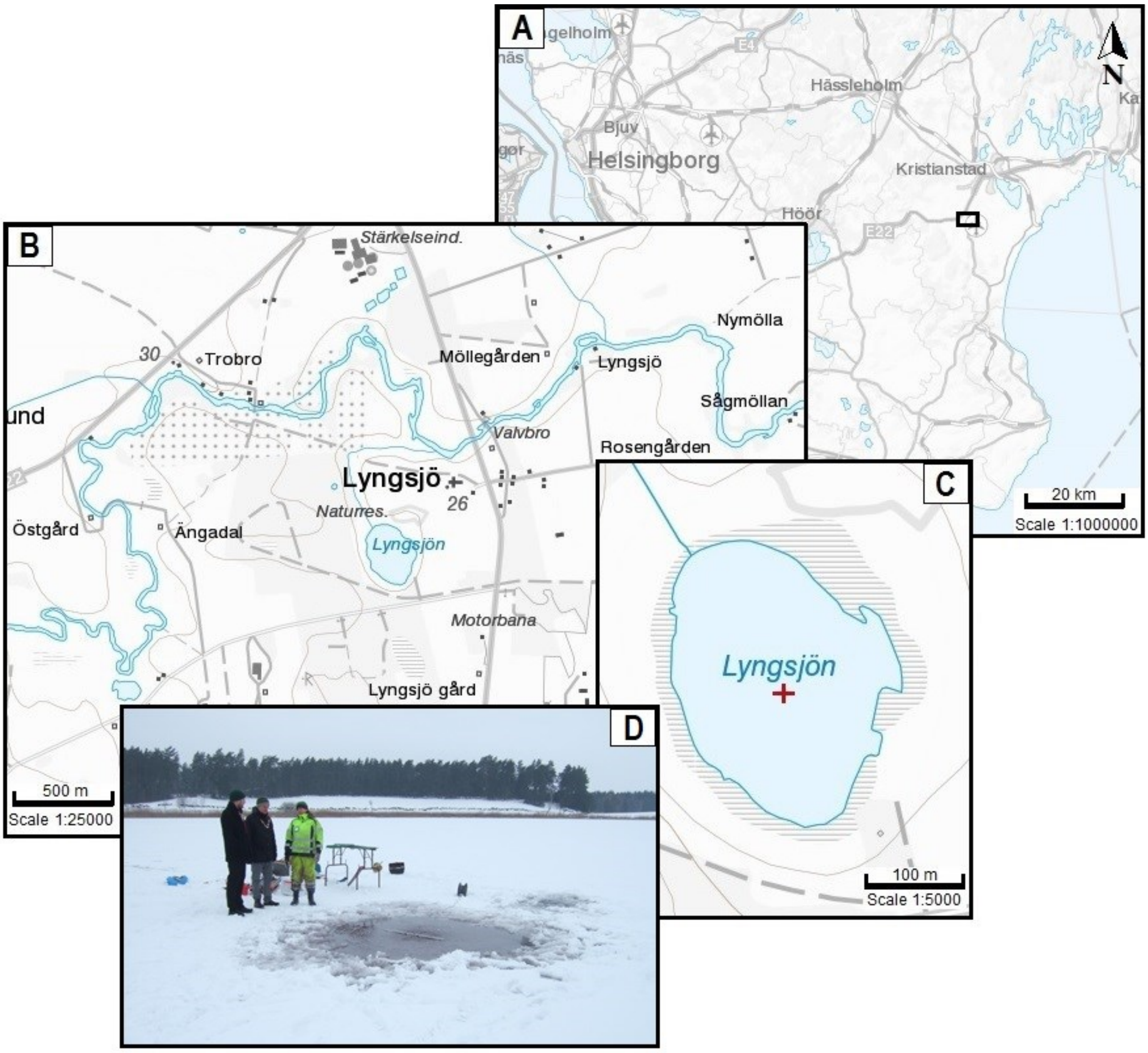

Fig. 1. The location of Lake Lyngsjön. A) Map of Scania (Sweden), the location of the lake is indicated by the small square. B) The local surroundings of Lake Lyngsjön, a narrow ditch can be seen connecting the lake with the Vramsån River, preventing the lake from flooding. The Lyngsjö village and church is situated approx. 300-400 meters northeast of the lake. C) The present outline of the lake. The coring point is indicated near the centre of the lake. Maps A-C are modified from the Geological Survey of Sweden (Quaternary map generator, Quaternary deposits, 2018). D) Fieldwork in February 2013. Note the present-day pine plantations west of the lake margin (Photo: Dan Hammarlund).

south of the lake, which is today overgrown by forest. The lake is today surrounded by sandy steppe vegetation on dry sandy fields where some of the fields are left fallow to preserve the characteristic vegetation (Swedish Environmental Protection Agency 2000).

The landscape is open to semi-open and characterized by sandy fields and pine plantations (Fig. 1D) with a land use consisting of both arable fields and pasture close to the lake (Lagerås 2004). Several remains and piles belonging to settlements from the Bronze Age have been found around the lake, indicating a long agricultural and cultural history at the site (County Administrative Board of Scania 2016).

2 Methods

2.1 Core collection and subsampling

Sediment cores for this study were collected in February 2013 from the central part of the lake. Core retrieval was conducted by Dan Hammarlund and Daniel Fredh from the Department of Geology at Lund University in collaboration with the National Historical Museums. The cores were obtained from the central part of the lake at a depth of 5 meters (lake bottom) using a Russian corer (1-meter core segments, 7.5 cm core diameter). The total sediment sequence obtained had a total length of 696 cm. The reference core sequence interval is indicated as 500 – 1196 cm (15 cores) where 500 cm represents the lake bottom sediment surface. Overlapping cores (approx. 40 cm overlap) were additionally retrieved from two parallel coring points for a complete stratigraphy. Furthermore, an 80 cm freeze core was retrieved covering the upper, most recent part of the stratigraphy. The Russian-core sequence was correlated and described in more detail by Allix Baxter as part of a student internship in 2015, and a lithostratigraphic description and division into

34 units was made.

For this study, sediments from the Russian-core reference sequence with overlapping cores were subsampled according to lithological boundaries into 2 cm segments covering a depth between 543 and 797.5 cm. The freeze core (500-579 cm) was also subsampled into 2 cm segments matching the resolution of the Russian-core sequence. 129 samples from the Russian-core sequence and 39 samples from the freeze core were subjected to geochemical analysis in addition to the quantification of aeolian sand. 4 samples from the deeper parts of the Russian-core sequence (outside of the study frame) were sampled for AMS ^{14}C radiocarbon dating and ^{210}Pb radioisotope dating was conducted on 15 samples from the upper 38 cm of the freeze core.

2.2 Quantification of mineral matter

Volumes of the samples from the Russian-core sequence were determined through water displacement. Volumes of freeze core samples were estimated by measuring the sides of the cuboid-shaped frozen samples with a ruler. This was found to be the optimal way to estimate the volume. An attempt to determine the volume through water displacement resulted in rapid thawing and considerable loss of sample material.

To be able to quantify the aeolian sand content, specifically the minerogenic grains of quartz and to some extent of carbonates, samples were wet-sieved using a 200 µm sieve. Samples from both core sequences were washed thoroughly until only mineral particles, carbonate shell fragments and plant fragments remained. The >200 µm material was transferred and stored in water-filled plastic containers and further examined under a light-microscope for extraction of carbonate shells. This was done to eliminate biogenic carbonate particles from the minerogenic residue.

Further on, the samples were carefully drained of excessive water and the residue was transferred to ceramic crucibles to be analysed for ignition residue (IR), to estimate the amount of minerogenic matter per unit volume of sediment, presumably of aeolian origin. Samples with large amounts of plant macrofossils were drained twice to remove the majority of the organic material and secondly for excessive water. Due to the difference in density between the macrofossils and the minerogenic component, the macrofossils remained in suspension for a longer time and the majority could be removed without the loss of mineral grains. The samples were ignited at 550°C for 4 hours and the previous removal of macrofossils was done to minimize the amount of ash produced after ignition.

The sedimentation rate (SR, cm year^{-1}) was calculated by dividing the sample thickness (the sample resolution) with the amount of years it took for the sample material to settle (years obtained from the age-depth model). The sand accumulation rate (SAR, g cm^{-2} year^{-1}) was calculated by multiplying the sedimentation rate (cm year^{-1}) with the mineral matter concentration (g cm^{-3}).

2.3 Geochemical analysis

Samples from both cores were analysed for carbon and nitrogen content by combustion in an elemental analyser (Costech ECS 4010). Freeze-dried samples were weighed in tin capsules for total carbon (TC) and total nitrogen (TN) content (%-weight). Samples were also analysed for total inorganic carbon (TIC) by treatment with 2M HCl acid for removal of carbonates according to Brodie et al. (2011). The samples for acid treatment were weighed in silver capsules and 10 µl distilled water was added to facilitate the reaction of HCl with carbonates as explained by Yamamuro & Kayanne (1995) and Brodie et al. (2011). Samples were kept on a hotplate at 50°C throughout the treatment and acid was added successively: 4x10 µl, 2x20 µl, 2x30 µl, 3x50 µl (approx. 280 µl total). The treatment was done continuously without letting the samples dry out and care was taken to avoid overflowing of the capsule contents due to the high carbonate contents of the sediments.

Approximately 40-50 samples were treated simultaneously and the last two acid additions of 50 µl were done to assure that all of the carbonates had been removed and no sign of foaming was noted. After treatment the samples were left to dry for approx. 3-4 hours on the hotplate followed by overnight drying in an oven at 105°C for complete acid removal. The dry silver capsule samples were folded and placed within tin capsules before being analysed (Brodie et al. 2011). The instrument was calibrated using Acetanilide as a standard. To check for drift during runs standards were run between every 10th sample.

The TIC content of the samples was calculated by subtracting the results of total carbon (TC) with total organic carbon (TOC) (Meyers & Teranes 2001; Enters et al. 2008). C/N atomic ratios were obtained by multiplying the C/N mass ratios by 1.167 in accordance with Meyers & Teranes (2001). The $CaCO_3$ (calcite content) percentage was calculated by multiplication of TIC values with 8.33 (Verardo et al. 1990; Enters et al. 2008).

2.4 Establishing the chronology

2.4.1 ^{210}Pb radioisotope dating

Freeze-dried samples from the freeze core (0-38 cm, 15 ^{210}Pb dates) were dated by direct gamma assay, and emitted gamma rays were measured to detect ^{226}Ra, ^{210}Pb, ^{137}Cs and ^{241}Am activity at the Environmental Radiometric Facility at University College London, England. The 'total' ^{210}Pb activity measured was subtracted by 'supported' (from *in situ* decay) ^{210}Pb activity to obtain the 'unsupported' (from the atmosphere) amount of ^{210}Pb (Appleby 2001).

To generate ^{210}Pb dates, the constant rate of supply (CRS) model was used, which assumes that the 'unsupported' ^{210}Pb is deposited at a constant rate and that the initial 'unsupported' ^{210}Pb deposited depends on changes in sedimentation rate and has not been disturbed after deposition resulting in a uniform decay of ^{210}Pb (Appleby 2001).

The radionuclides of ^{137}Cs and ^{241}Am (artificially produced) were used to correct the ^{210}Pb chronology, assuming that the radionuclides were generated from the testing of nuclear weapons (peak in atmospheric fallout in 1963) (Appleby 2001).

2.4.2 Radiocarbon dating

Four samples from the Russian-core sequence were wet-sieved and terrestrial macroscopic plant remains were picked out for AMS ^{14}C dating (conducted at the Radiocarbon Dating Laboratory at Lund University, Sweden). Calibration of the radiocarbon dates was performed with IntCal13.14C calibration curve (Reimer et al. 2013), which is used for Northern Hemisphere terrestrial dates (Blaauw 2010). For the construction of the age-depth model and calibration, Clam (version 2.2, Blaauw 2010) using the software R (version 3.3.2, R Development Core Team 2016) was used. In addition, 10 ^{14}C ages previously sampled from the Russian core sequence, were calibrated together with the four ^{14}C ages generated for this project.

2.4.3 Age-depth model

The Clam code creates 'classical age-depth models' which are non-Bayesian (Blaauw 2010). A stable lake environment without any hiatuses in the sediment deposition was assumed for Lake Lyngsjön and smooth spline functions (smooth spline (type=4) and smooth (smooth=0.8)), were applied for the age-depth model (Blaauw 2010). A total of 14 ^{14}C ages and 15 ^{210}Pb ages were used to construct an age-depth model for the sediment sequence.

2.5 Pollen analysis

Pollen analysis of samples from the Russian-core sequence was conducted by Leif Björkman as part of an ongoing infrastructure archaeology contract (see Björkman (2018) for methods and complete reconstructed pollen record). A few selected taxa were permitted for use in this project as an additional support to the interpretation of aeolian sand drift events and geochemical changes inferred from the sediment record. The selected pollen taxa used for this project are presented as percentages of the total pollen sum, representing more than 1100 pollen grains per sample identified as pollen from trees, shrubs, grasses and herbs.

Diagrams presenting the results of the aeolian sand accumulation rate (ASAR), SR, geochemical data, population data and pollen data were constructed using the C2 software, version 1.7.6 (Juggins 2007).

3 Results

3.1 Sediment description and core correlation

The sediment sequence studied consists of calcareous gyttja, which has been visually divided into three different types of hues (medium brown, medium-dark brown and dark brown) (Table 1). Unit 33 (medium brown) was used to visually correlate the Russian-core sequence to the freeze core prior to subsampling (Fig. 2). This unit was later determined to contain the highest measured amounts of aeolian sand. Geochemical analysis of both core sequences revealed a slight mismatch in the initially established depths and a slight shift of 4 cm upwards of the Russian core sequence created an almost perfect fit based primarily on the C/N ratios. The correlation was done on 20 overlapping samples.

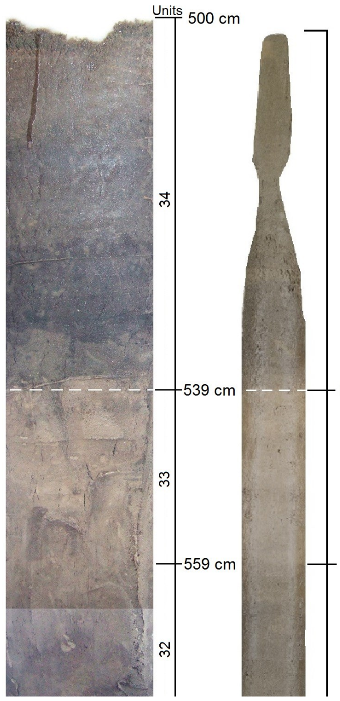

Fig. 2. Correlation between the Russian-core sequence (right) and the freeze core (left). Unit 33 (sandy calcareous gyttja), was used to initially correct depths of the Russian-core sequence. Unit 33 contains the highest quantity of aeolian sand deposited throughout the studied sediment succession.

Table 1. Lithostratigraphic description of the sediment sequence from Lake Lyngsjön. Units 34-23 represent the sediment interval 500-793.5 cm analysed for this project. Information regarding units 22-1 was not included due to them being outside the scope of this project. The sediment description below, initially provided by Allix Baxter, was corrected after geochemical analysis.

Depth interval (cm)	Units	Sediment colour	Sediment description
500-539	34	Medium-dark brown	Calcareous gyttja
539-559	33	Medium brown	Sandy calcareous gyttja
559-589	32	Medium-dark brown	Calcareous gyttja
589-613	31	Dark brown	Calcareous gyttja
613-631	30	Medium-dark brown	Calcareous gyttja
631-672	29	Dark brown	Calcareous gyttja
672-683.5	28	Medium-dark brown	Calcareous gyttja
683.5-698.5	27	Dark brown	Calcareous gyttja
698.5-704	26	Medium-dark brown	Calcareous gyttja
704-756	25	Dark brown	Calcareous gyttja
756-775.5	24	Medium-dark brown	Calcareous gyttja
775.5-793.5	23	Medium-dark brown	Calcareous gyttja

3.2 Chronology

3.2.1 ^{210}Pb dating and artifical radionuclides

The unsupported ^{210}Pb activity changes irregularly from 1.5 cm (407.69 Bq Kg^{-1}) down to 37 cm (10.28 Bq Kg^{-1}) (Fig. 3A). The upper part of the record (1.5 to 27 cm) shows an almost stepwise decrease in unsupported ^{210}Pb while the lower part (27 to 37 cm) shows a more rapid decrease in unsupported ^{210}Pb activities with depth. The ^{137}Cs activity peaks around 27 cm (42.56 Bq Kg^{-1} at 26 cm, 38.73 Bq Kg^{-1} at 28 cm) (Fig. 3B). The additional presence of ^{241}Am at 26 cm and 28 cm indicates that the ^{137}Cs peak is probably a product of the 1963 testing of nuclear weapons (Appleby 2001) (Fig. 3B). The depth of 27 cm was assigned as the year 1963 to correct the ^{210}Pb chronology. Additional information regarding the ^{210}Pb chronology can be seen in Appendix 1.

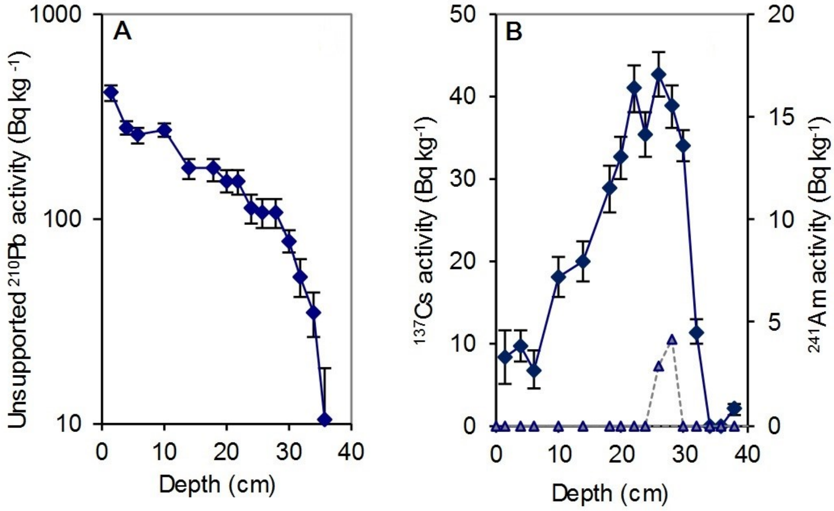

Fig. 3. Concentrations of ^{210}Pb and artificial radionuclides of ^{137}Cs and ^{241}Am from the freeze core. A). Unsupported ^{210}Pb. B). ^{137}Cs activity (upper graph) and ^{241}Am activity (lower graph, shown by triangles).

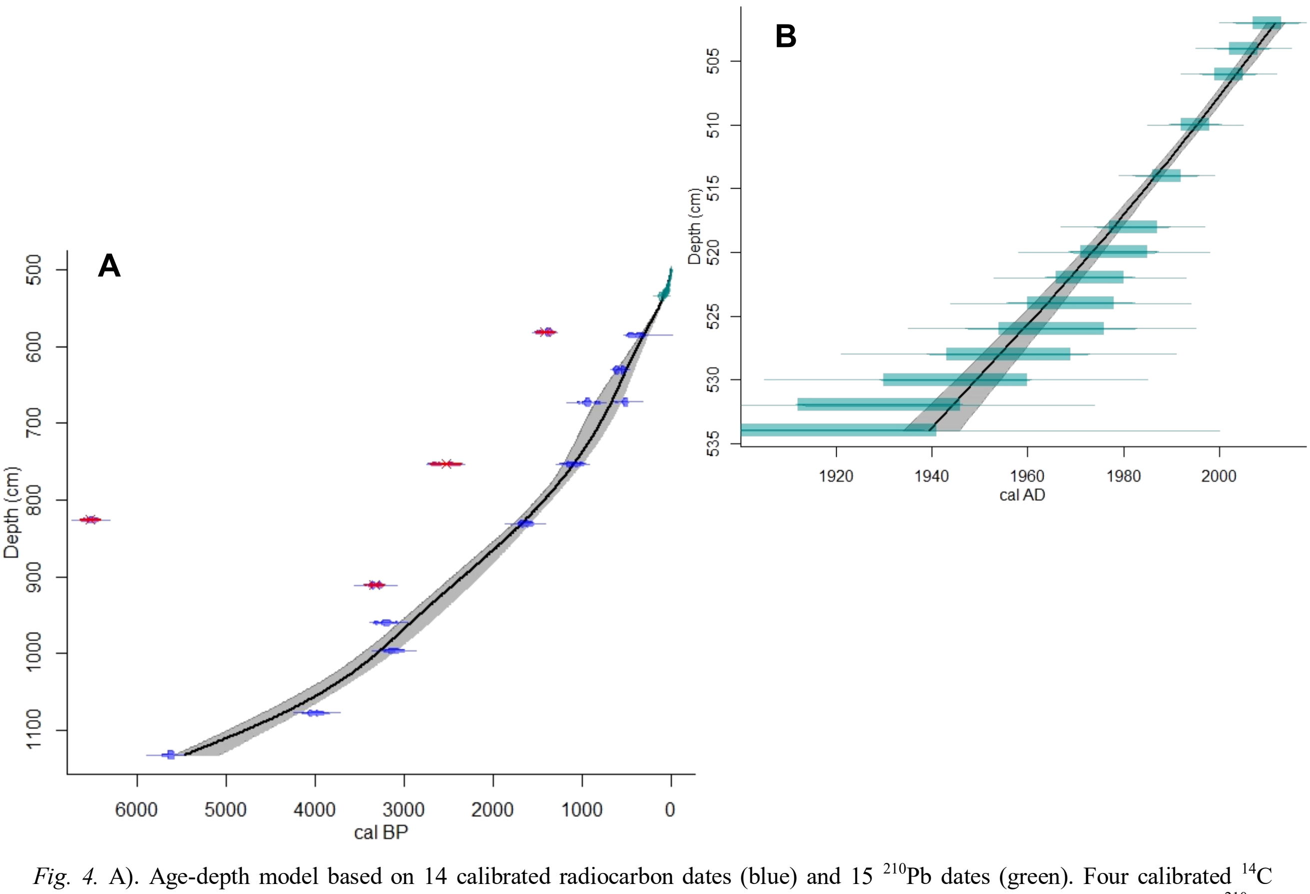

Fig. 4. A). Age-depth model based on 14 calibrated radiocarbon dates (blue) and 15 ^{210}Pb dates (green). Four calibrated ^{14}C dates are marked as outliers (crossed red). The shading represents confidence intervals of 95% (2σ-range). B). The 15 ^{210}Pb dates from the upper part of the age-depth model.

Table 2. Results obtained from radiocarbon dating. Dated material represents plant macrofossils used. 2σ-range represents 95% confidence interval of calibrated ages. Lab. numbers marked with an 'a' were done for this project. Lab. numbers marked with an asterisk (*) represent outliers in the age-depth model.

Lab. number	Depth interval (cm)	Dated material	^{14}C age BP	2σ –range (cal BP)
LuS-11492*	580-583	10 plant macrof.	1505 ± 40	1311-1521
LuS-11928	583-588	1 wood, 1 herb stem, 1 *Betula* seed	350 ± 45	312-495
LuS-11491	628-632	10 plant macrof.	565 ± 45	518-651
LuS-11929	672-672	1 wood	485 ± 35	492-616
LuS-11490	671-674	15 plant macrof.	1025 ± 40	801-1052
LuS-11930	751-755	1 wood, 1 *Rubus idaeus*, 1 *Potamogeton*, 1 *Carex*, 1 *Potentilla*	1175 ± 45	976-1231
LuS-11489*	751-755	1 *Carex*, 2 wood, 10 plant macrof.	2450 ± 45	2360-2705
LuS-11488*	824-828	9 reed macrof.	5725 ± 40	6415-6635
LuS-11931	828-834	2 brownmoss, 1 bud scale	1730 ± 40	1549-1725
LuS-12123[a]*	897-912.5	1 *Pinus* bark, 1 bud scale, *Betula* fruit, wood fragments	3120 ± 40	3229-3443
LuS-11487	958-962	1 *Alnus* seed, 10 plant macrof.	3015 ± 35	3078-3339
LuS-12122[a]	990.5-1000.5	1 *Rumex* seed, 1 bud scale, 1 *Betula* fruit	2960 ± 40	2988-3234
LuS-12121[a]	1072-1084	1 *Betula* catkin, 1 *Alnus* cone, 1 bud scale, 1 bark fragm, seeds	3670 ± 40	3890-4142
LuS-12120[a]	1126-1135.5	1 *Pinus* bark, 1 *Alnus* cone, leaves	4895 ± 40	5586-5714

3.2.2 Age-depth model

A total of 14 ^{14}C ages were calibrated, 10 of which were used to construct the age-depth model while four were considered as outliers based on their anomalously high ages (Fig. 4A). To complete the upper part of the chronology, 15 ^{210}Pb dates were added to the age-depth model (Fig. 4A and B). The age-depth model is based on a smooth spline curve with 95% confidence intervals (default in Clam) and min-max age ranges for each ^{14}C date. Detailed information regarding depths, macrofossils and min-max ages of the calibrated ^{14}C ages are presented in Table 2.

3.3 Aeolian sand content

The sand accumulation rate, which is assumed to represent primarily deposition of aeolian sand (aeolian sand accumulation rate, ASAR) together with the geochemical data can be seen in Fig. 5. divided into six zones based on changes recognized in the geochemical data and aeolian sand deposition. The reconstructed sequence begins around AD 650 with almost no deposition of aeolian sand between AD 650 and AD 780. The following 185 years are characterized by a steady increase in deposition of aeolian sand until AD 965 where the amount of sand reaches up to 0.0004 g cm^{-2} $year^{-1}$. Another noticeable peak can be seen around AD 1170 with re-occurring higher amounts of sand (almost 0.0003 g cm^{-2} $year^{-1}$). The 1170s peak is followed by another period of lowered deposition of aeolian sand seen as minor peaks until AD 1410 where a second major peak can be seen with values once more reaching up to 0.0004 g cm^{-2} $year^{-1}$.

Two minor peaks around AD 1540 and AD 1590 with noteworthy sand content appear after a period of lowered deposition of sand which lasted for approximately 100 years. The onset of the 18^{th} century is characterized by two prominent peaks based on two samples with very little material (mostly organic matter) and their significance will be discussed later. The peak around AD 1840 can be disregarded due to clay being encountered in the sample after ignition. A third and most prominent major peak can be seen at the onset of the 20^{th} century with values reaching up to 0.0008 g cm^{-2} $year^{-1}$ around AD 1920. This increase in aeolian sand deposition involves 8 samples with noticeable amounts of sand measured and covers approximately 50 years. The aeolian sand deposition history at the site is concluded with a minor peak occurring after the onset of the 21^{st} century.

Detailed information regarding sample volumes, IR weights, mineral matter concentration, SR and ASAR can be found in Appendix 2.

3.4 Sedimentation rates

The sedimentation rate (SR, cm $year^{-1}$) throughout the majority of the sequence studied changes only slightly (Fig. 5). In the deepest part of the sequence (around AD 650) the sedimentation rate gradually increases from 0.1 cm $year^{-1}$ up to 0.2 cm $year^{-1}$ around the 14^{th} century AD. The sedimentation rate increases to a maximum of 0.3 cm $year^{-1}$ around AD 1450 before it decreases to 0.2 cm $year^{-1}$ between AD 1700 and AD 1800. The sedimentation rate reaches a maximum during the last 150 years, from 0.2 cm $year^{-1}$ to 1 cm $year^{-1}$ at the top. This is probably due to high water content and overall less compacted sediments towards the surface compared to the deeper parts of the sequence. The topmost sample has a resolution of 3 cm (from the freeze core) with loosely packed sediments, which could explain the exceptionally high value of 1 cm $year^{-1}$.

The sedimentation rates can be described as unusually high (pers. com. Dan Hammarlund), and the sediment sequence encompasses only a fraction of the post -glacial lake history.

3.5 Geochemical data

Results for both core sequences are presented in Fig. 5 where data from the freeze core and the Russian-core sequence are indicated by blue and red respectively.

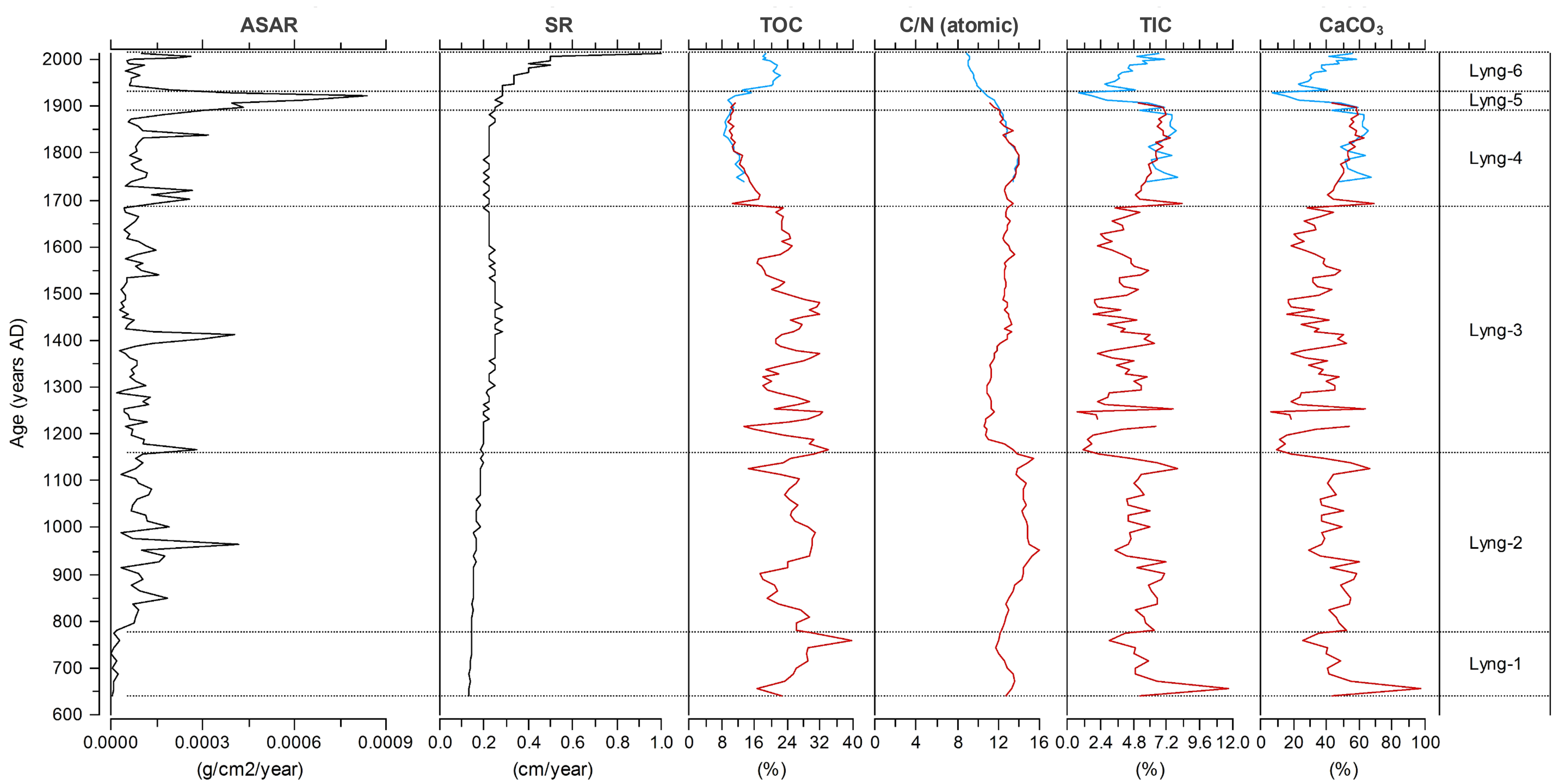

Fig. 5. Records of total organic carbon (TOC %), C/N ratio (atomic), total inorganic carbon (TIC %) and calcium carbonate ($CaCO_3$ %) with results from the freeze core (blue, upper) and Russian-core (red, lower). The quantified aeolian sand (aeolian sand accumulation rate, ASAR), represented as sediment accumulation rates (g cm^{-2} year^{-1}) and the sedimentation rate (SR, cm year^{-1}) represent a continuation of both cores sequences where the upper part is solely based on analysis on the freeze core. All records are plotted against age expressed as calibrated years AD (linear time scale) and divided into six zones based on visual changes in geochemical data and aeolian sand deposition.

Values of TOC and TIC are generally anti-correlated, which can be seen for the majority of the succession. The largest variations in TOC and TIC occur between AD 650 and AD 1700. A gradual change in TOC and TIC can be seen after the 18th century followed by a sharp decrease in TIC values after the onset of the 20th century. The declines in both TOC and TIC are followed by a sharp increase in TOC and a more gradual increase in TIC around the 1930s and onwards. Maximum TOC values of 40% can be seen around AD 750 and minimum values of 9% occur around AD 1840. TIC reaches up to 12% at onset of the succession and minimum values of 1% can be seen around AD 1250 and AD 1930 respectively.

C/N atomic ratios vary less drastically compared to TOC values. The C/N ratios range from values close to 9 at the very top of the profile (lowest value), to values of 16 around AD 950 (highest value) (Fig. 5). C/N ratios are elevated between AD 950 and AD 1150. A rather rapid transition to lower values (approx. 11) occurs at the end of the 12th century and lasts throughout the 13th century. C/N ratios gradually increase up to 13 between 1750 and 1820 followed by a steady decrease into the 21st century.

A gap in the TIC and $CaCO_3$ profiles can be seen around AD 1220, this is due to the removal of one sample indicating a negative TIC value. Changes in $CaCO_3$ are used to determine the type of sediments deposited. Sediments containing approximately 20-80% $CaCO_3$ are referred to as calcareous gyttja (Wesenbeeg-Lund 1901).

3.6 Population of Lyngsjö Parish

Population data for the Lyngsjö Parish can be seen in Fig. 6. The population graphs are based on data from Andersson Palm (2000) (year 1571 to 1900) and from Holmstedt (1956) (year 1862 to 1955) coloured red and blue respectively. The population numbers remain below 200 between AD 1571 and AD 1620. Following these years the population gradually increases and reaches a population maximum of 448 (AD 1869) after which the population decreases down to 243 as recorded for AD 1955. Minor differences in the population graphs can be seen for the period between 1860 and 1900. These differences are mainly due to the data resolution and both datasets point towards an overall decline in population, which can be seen after the population maximum. Population data from AD 1751 are estimated on an average from neighbouring areas and their household sizes (Andersson Palm 2000).

3.7 Pollen data

The pollen taxa used for this project are presented in Fig. 7. The following taxa were selected: the tree types birch (*Betula*), pine (*Pinus*), beech (*Fagus*) and spruce (*Picea*), the shrub taxon juniper (*Juniperus*), the herb types oat (*Avena*), barley (*Hordeum*-group), rye (*Secale*), wheat (*Triticum*), mugwort and wormwood (*Artemisia*), hemp and hop (*Cannabis*-type), ribwort plantain (*Plantago lanceolata*) and sorrel (*Rumex acetosa*/*Rumex acetosella*). The green algae *Pediastrum* was also included. The pollen diagram was divided into zones based on the zonation defined for aeolian sand accumulation rate (ASAR) and geochemical data.

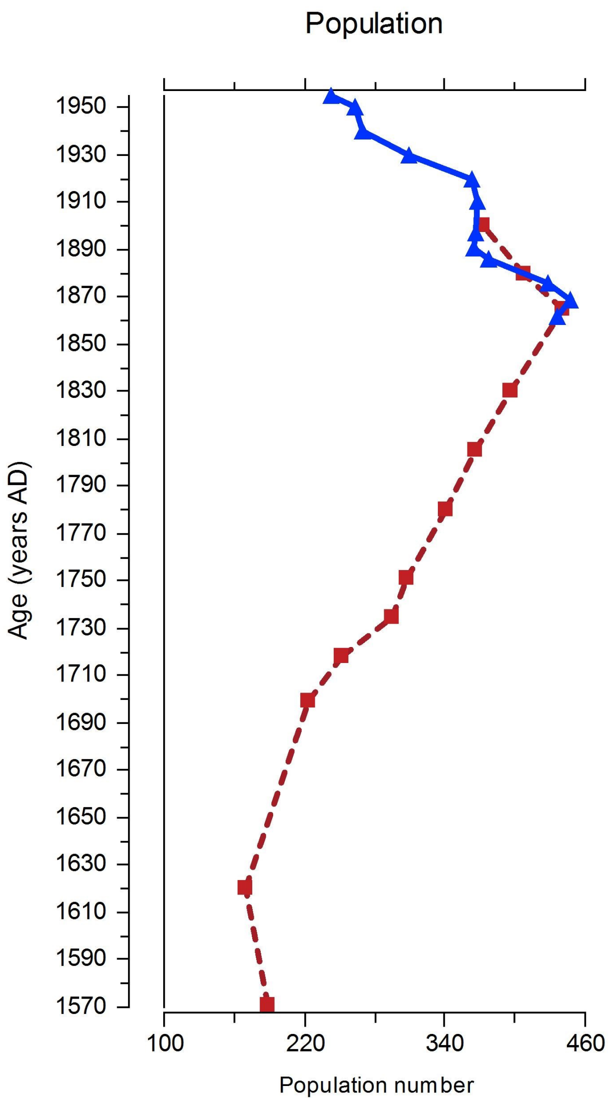

Fig. 6. Population data for Lyngsjö Parish based on data from Andersson Palm (2000) and Holmstedt (1956). Data from Andersson Palm (2000) are shown by red squares (1571 to 1900) and data from Holmstedt (1956) are shown by blue triangles (1862 to 1955).

4 Discussion

4.1 Human impact, aeolian activity and sediment geochemistry

Here the aeolian sand deposited during the last millennium as presented in Fig. 5 and divided into six zones will be further connected to historical events and changes in human land use close to the lake. The geochemical changes are used to help interpret lake sediment development as well as recognize input of terrestrial organic matter from human disturbances in proximity to the lake. Pollen percentages of selected pollen types indicative of cultivation and landscape openness (Fig. 7), are used to evaluate whether aeolian sand transportation has been facilitated during extensive

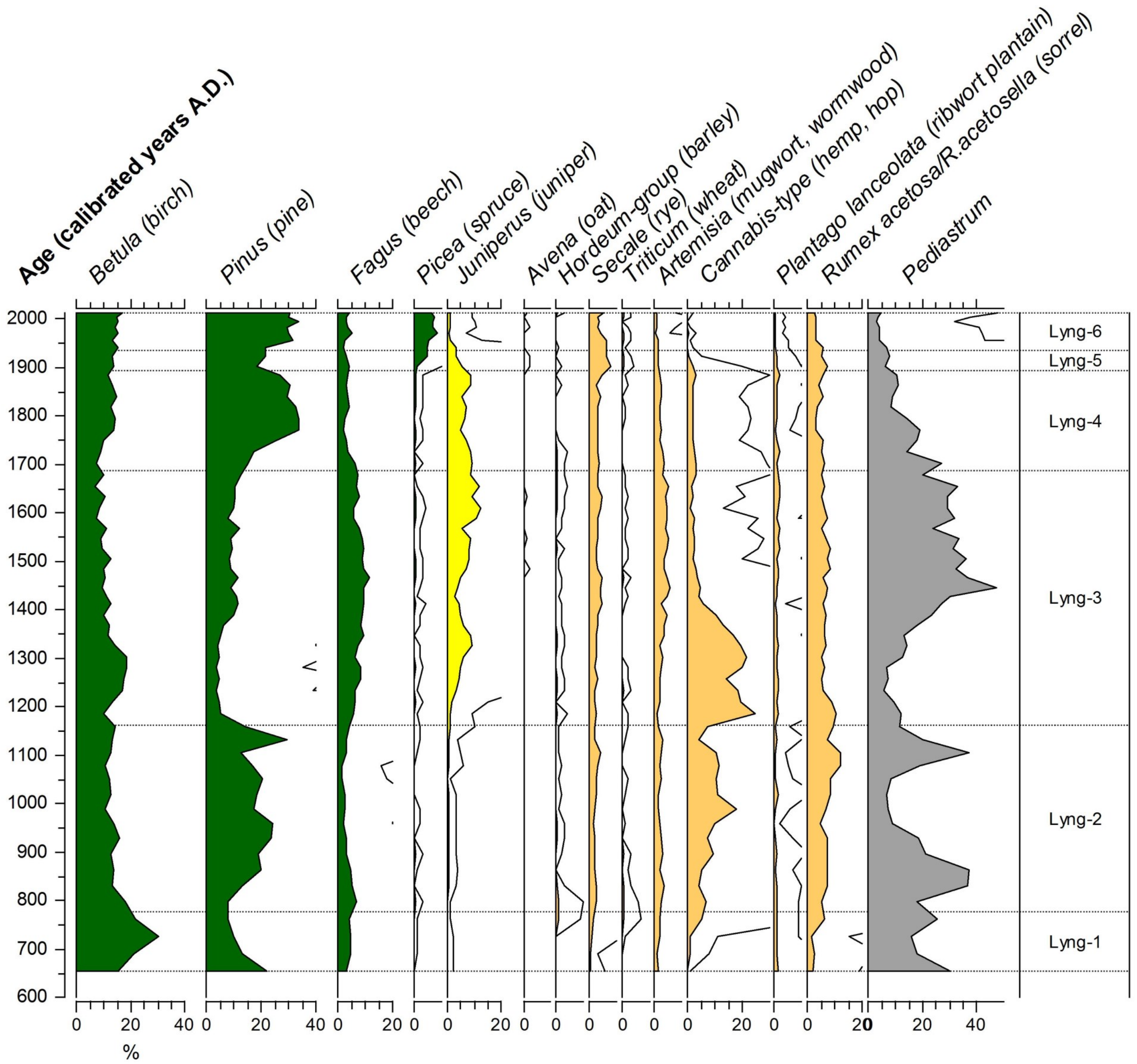

Fig. 7. Pollen diagram showing trees, shrubs, herbs and *Pediastrum* algae. Pollen types are based on percentages of the total pollen sum, and zones follow the geochemical and aeolian sand accumulation rate (ASAR) zonations. All pollen types are plotted against modelled ages expressed as calibrated years AD (linear time scale) and finer lines represent x10 exaggeration of pollen percentages.

periods of cultivation and minimum forest cover. Historical maps offer a coarse estimate of agriculture versus forest coverage both locally and regionally and will be used to further describe the aeolian activity around the lake.

4.1.1 Lyng-1 (AD 640-770)

The aeolian sand content for this time interval is very low. TOC values reach highest measured (40%) and a strong anti-correlation with TIC values can be seen. The highest TIC value (12% TIC, 97% $CaCO_3$) at the onset of this zone can be related to high carbonate content, probably derived from high amounts of shell-fragments in samples (shells recognised as produced in the lake). C/N ratios around 12 indicate aquatic productivity as the main source of organic matter for this zone (Meyers & Teranes 2001). The lower C/N ratio (below 12) towards the upper part of the zone which coincides with high TOC (40%) confirms algal productivity being dominant (e.g. Routh et al. 2004).

The relatively high percentages (approximately 20%) of *Pediastrum* (green algae), which is indicative of increased input of nutrients into the lake and a subsequent increase in lake productivity, may reflect human disturbance around Lake Lyngsjön (Bradshaw et al. 2005; Li et al. 2008; Rasmussen & Olsen 2009).

Past human disturbance in the area can also be inferred from the pollen diagram (Fig. 7) with the presence of pollen indicating cultivation (*Secale* (rye), *Triticum* (wheat), *Hordeum* (barley) and *Cannabis*-type (hemp, hop)) and pasturage (*Plantago lanceolata* (ribwort plantain) and *Rumex acetosa/Rumex acetosella* (sorrel)) during the 8th century and onwards together with disturbance favoured *Artemisia* (mugwort, wormwood) (e.g. Behre 1981; Gaillard & Berglund 1988; Gaillard et al. 1991a, 1991b; Lagerås 1996, 2007). What can be further noted is the presence of trees during this zone, mostly *Betula* (birch) and somewhat lesser abundances of *Pinus* (pine) and *Fagus* (beech) which could have partially hampered the transportation of aeolian sand into the lake (Enters et al. 2010).

4.1.2 Lyng-2 (AD 770-1160)

A trend with increased aeolian activity can be seen beginning around AD 780 and ending with a major peak at AD 965 (Fig. 5). Simultaneously, TOC decreases successively as compared to an increase in TIC. The decreasing TOC content seen could have been due to dilution by minerogenic matter of aeolian origin (Meyers & Lallier-Vergès 1999; Meyers 2003; Enters et al. 2006), with addition of carbonates from soils which increased TIC (Enters et al. 2010). An increase in *Pediastrum* algae (Fig. 7) may reflect increased nutrient delivery related to these processes (Bradshaw et al. 2005; Li et al. 2008).

C/N ratios increase steadily up to a peak value of 16 (AD 950) which points toward increasing input of terrestrial organic matter caused by human disturbance, probably agricultural activity that led to some transportation of tree debris from nearby forests (Kaushal & Binford 1999; Barnekow et al. 2008).

A rather sharp and lasting increase in TOC values coincides with the peak recorded in C/N ratios. This event is reflected by a sharp decrease in TIC, a significant input of aeolian sand (major peak in aeolian sand recorded at AD 965) and increased TOC. The higher C/N ratio confirms predominantly terrestrial organic matter being transported into the lake (Meyers & Lallier-Vergès 1999), with reduced algal productivity and low nutrient input (low *Pediastrum*) (Li et al. 2008). The decrease in TIC can be explained by: 1) dilution by terrestrial organic matter (Dean 1999; Enters et al. 2010), and 2) carbonate-producing algae (*Chara*-type) being negatively affected by a major input of aeolian sand leading to lowered TIC values (Hammarlund et al. 2005). What should also be noted is the increase in pine pollen in this zone and relatively high and stable birch pollen frequencies, indicating the presence of trees in the area as a possible contributor of terrestrial organic matter and elevated C/N ratios (Wolfe et al. 1999; Enters et al. 2006). Although the presence of trees explains the higher C/N ratios, the increase in aeolian sand transported into the lake does not seem to have been affected by increasing forest cover.

Following the major peak in aeolian sand content at approx. AD 965 is a period of reduced aeolian sand drift with minor impact on TIC and TOC. TOC declines and reaches a value below 15% (onset of 1100s) and at the same time TIC increases to approximately 8%. The decreasing TOC values do not seem to have a corresponding effect on the C/N ratios which remain around 14 (from approximately AD 1000) until C/N ratios increases (up to 16) just below the upper zone boundary. C/N ratios of 12-14 indicate a mix of terrestrial and algal organic matter, and higher values indicate an enhanced contribution of terrestrial material into the lake (Meyers & Lallier-Vergès 1999; Meyers & Teranes 2001; Enters et al. 2010).

Increased catchment erosion could have contributed to increased *Pediastrum* algae in the lake (Li et al. 2008; Rasmussen & Olsen 2009), diluting TOC and contributing with terrestrial organic matter causing a second peak in C/N ratios (AD 1150) (Enters et al. 2006). Enhanced input of vascular plants would have been due to deforestation close to the lake, just before AD 1160, which corresponds to elevated C/N ratios close to 16 (Kaushal & Binford 1999), and coincides with an increase in TOC content towards the upper zone boundary. This is also inferred from the pollen diagram with pine pollen percentages decreasing before the zone transition.

During the 12th century, the Lyngsjö church was built (Sallerfors 1974). Although settlements at Lyngsjö occurred long before the introduction of Christianity (Holmstedt 1956), the church could perhaps have brought a period of increased settlement in the area close to the lake, which could have initiated the deforestation recorded.

4.1.3 Lyng-3 (AD 1160-1680)

A noticeable peak in aeolian sand content appears slightly after the inferred deforestation event occurring just before AD 1160 as recorded by elevated C/N ratios and decreasing pine pollen percentages (Figs. 5, 7). This coincides with an opening of the landscape which would have facilitated transportation of aeolian sand (Agrell 1981; de Jong et al. 2006; Breshears et al. 2009). In connection to this event, C/N ratios gradually decrease (C/N ratio approximately 11) indicating a shift towards mainly algal productivity in the lake (Meyers & Lallier-Vergès 1999). After the deforestation, the main source of terrestrial organic matter would have been removed and therefore leading to gradually decreasing C/N ratios with the dominant source of organic matter becoming algal (Enters et al. 2006). The substantial decrease in TIC content probably reflects *Chara*-type algae being disturbed by an increase in suspension load (mainly aeolian sand, AD 1170) (Nõges et al. 2003; Hammarlund et al. 2005).

Decreasing *Pediastrum* abundances seem to coincide with the deforestation event, although decreased input of nutrients due to minor catchment erosion caused by changes in land use is a more likely explanation. The opening of the landscape as inferred from the pollen diagram is mostly seen as a reduction in pine, followed by subtle increases in beech and birch pollen abundances. Simultaneously, juniper (*Juniperus*) increases and becomes more abundant than before the deforestation. This might be a result of diminishing tree cover, promoting the expansion of light-demanding shrubs such as juniper, which could additionally have been retained as construction material by settlers (Lagerås 2007).

The shift to lower C/N ratios persists for approximately 200 years when aeolian sand input was generally low and appear to have had little impact on TOC and TIC changes. Although aeolian sand contribution varies, sedimentation rates during this zone are slightly higher than previously (from 0.2 cm year^{-1} at AD 1200 to 0.29 cm year^{-1} around AD 1420-1460), indicating increased contribution of minerogenic matter possibly due to catchment erosion and input of aeolian sand (Enters et al. 2010). What can be additionally noted from the pollen diagram is the increase in *Cannabis*-type (hemp, hop) pollen. *Cannabis*-type pollen has been present since zone 1 (Lyng-1) with some note-

Fig. 8. Excerpt from Gerhard von Buhrman's map over Scania established in 1684. The map depicts Lake Lyngsjön (indicated by a red square) in an open to semi-open landscape with the closest forests located near Lyngby and northeast of the lake, across the Vramsån River. The original map is preserved at the Swedish Military Archive in Stockholm (Part of Karl XI Kungsboken 1655-1735, available through the Swedish National Archive website). Approximate scale of the original map: 1:200 000.

worthy abundances throughout zone 2 (Lyng-2) and reaching percentages exceeding 20% just before the 13th century. These higher percentages point towards a period of hemp retting having occurred in the lake for production of e.g. ropes (Lagerås 2007). This process involves soaking of stems (in this case hemp stems), which contributed to the amplified pollen percentages seen (Rasmussen & Anderson 2005; Lagerås 2007). What should also be noted is that the 'agrarian crisis' during the 14th century (Berglund 2007), did not have a major impact on the Lyngsjö area. This is mainly seen in the pollen diagram, displaying a continuous presence of pollen indicative of cultivation and pasturage, similar to Bjäresjösjön (southern Scania) (Gaillard et al. 1991a).

A major peak in aeolian sand content occurs at the beginning of the 15th century. TOC does not seem to be diluted by minerogenic input and TIC reflects algal *Chara*-type community being temporarily disturbed. Following this major aeolian peak is an increase in C/N ratios (values up to 13) which implies contribution of terrestrial organic matter due to enhanced soil erosion or extensive agricultural activity close to the lake (Meyers 2003; Barnekow et al. 2008; Enters et al. 2010). A peak in *Pediastrum* seems to coincide with this event, confirming the elevated catchment erosion (Rasmussen & Olsen 2009). Hemp retting appears to cease right before the major peak in aeolian sand content. According to Agrell (1981), aeolian activity seems to have increased during the 14th century as a result of increased forest clearing and cultivation southeast and northeast of Lyngsjö (areas of Vittskövle and Trolle-Ljungby). The aeolian sand peak recorded at the onset of the 15th century at Lake Lyngsjön could well be the result of culminating aeolian activity occurring regionally in eastern Scania as a result of a deforestation event (opening of the landscape).

Following the 15th century major peak, a period of lower aeolian activity took place, except for two minor peaks during the 16th century. These minor peaks appear to have no noticeable impact on the TOC and TIC contents. C/N ratios remain between 12 and 13 for the continuing part of the zone, indicating a mix of algal and terrestrial organic matter (Meyer & Lallier-Vergés 1999; Meyers & Teranes 2001). This change towards stable C/N ratios is followed by continuously high frequencies of *Pediastrum* and a minor increase in tree pollen frequencies, primarily pine and beech. The area

Fig. 9. Lake Lyngsjön and its local surroundings as portrayed in 1803 before the 'enskifte' agricultural changes. The map depicts land use through arable fields and pastures. No forests are present locally. Map from Lantmäteriet's Historical Archive of Maps.

around Lyngsjön was characterized by poor soils due to sand drift during the 16th century (Sallerfors 1974). The late 16th century to late 17th century is described as years with low agricultural productivity due to sand drift caused by forest clearance as retold by Regnéll (1980). What is also noted is that obstacles such as parcel fences were scarce (Regnéll 1980), which could have contributed to some aeolian sand being transported into the lake during the 16th century.

The onset of the 17th century was characterized by war with the main road through Lyngsjö village being used as a passage for soldiers (Sallerfors 1974). It is also possible that parts of the Lyngsjö village during later conflicts would have been affected by fires in connection with the war (Holmstedt 1956; Sallerfors 1974), although no clear indications for this can be seen in the geochemical and pollen data.

The agricultural productivity in the area belonging to Lyngsjö village in 1671 is explained by Sallerfors (1974) and Regnéll (1980) as slightly worse due to increased sand drift compared to 100 years earlier. This is slightly conflicting with the aeolian sand record for the 17th century, which indicates lower aeolian activity compared to the 16th century. It can also be noted that there are no forests belonging to the Lyngsjö village in 1671 (Sallerfors 1974), although it is still possible that forests may have been present at a distance from the lake. The population of the Lyngsjö Parish decreased from 189 individuals in 1571 to 170 in 1620, which is most likely due to the war and has increased steadily afterwards (Fig. 6) (Andersson Palm 2000).

4.1.4 Lyng-4 (AD 1680-1890)

A trend towards lower TOC values and gradually increasing TIC values is characteristic for this zone. At the same time C/N ratios increase slightly (up to 14) and remain elevated between AD 1740 and 1810. The decline in TOC values in combination with enhanced C/N ratios can be explained by enhanced catchment erosion diluting the TOC content (Meyers & Lallier-Vergés 1999; Barnekow et al. 2008). The increase in TIC content is probably related to increased productivity by *Chara* algae in the lake (Hammarlund et al. 2005), combined with increased input of terrestrial carbonates (Enters et al. 2010). Within this zone, a considerable increase in pine along with a subtle increase in birch can be seen from the 1760s and onwards. The increase in C/N ratios seems to coincide with a rise in tree pollen, indicating some terrestrial input of organic matter due to increased forest cover close to the lake (Enters et al. 2006). The onset of the 18th century before the increase in pine and birch pollen is characterized by an increase in aeolian sand deposition, followed by a period of relatively low aeolian activity between AD 1730 and 1860.

The villages of Lyngsjö and Hommentorp (a village west of Lyngsjö) had according to Regnéll (1980) as inferred from Gerhard von Buhrman's map (year 1684), no forests in proximity to the lake. The only forests mentioned are pinewoods close to Lyngby (south of Lyngsjö), and deducing from Buhrman's map, there was also a small forest north-east of Lyngsjö (Fig. 8) (Regnéll 1980). The village is de-

Fig. 10. Lake Lyngsjön as depicted in 1826, after the implementation of the 'enskiftet' land amalgamation. According to Regnéll (1980) the lake was twice the size compared to his observations in the 1970s. An overgrown smaller lake named Älvasjön is located south of Lake Lyngsjön. Map from Lantmäteriet's Historical Archive of Maps.

scribed as devoid of forest by Anders Tidström in 1756 who also mentions sandy fields close to the Lyngsjö church on his journey through Scania (Weibull 1891). A regional rise in aeolian activity occurred on the Kristianstad Plain at the beginning of the 18th century and lasted until the onset of the 19th century before the implementation of land amalgamation ('enskiftet' in Swedish) (Agrell 1980, 1981; Bärring et al. 2003; Olsenius 2014). Simultaneously, the increase in sand deposition recorded during the 18th century can be linked to intensified agricultural land use at a regional scale (Agrell 1980). During this phase, several sand dunes started to form. Two dunes relatively close to Lake Lyngsjön began to form in 1750s in the area of Gringelstad (east of Lyngsjö) and Åkeslund (south-east of Lyngsjö) according to Olsenius (2014). Two additional dunes located further south to south-east of the lake, in the area of Eskilstorp and Vittskövle began forming around AD 1735, slightly earlier than the dunes closest to the lake (Olsenius 2014). However, recent dating of the Vittskövle dune revealed that it was formed during the period of AD 1686-1724, indicating that aeolian activity must have occurred even earlier in the southern parts of the Kristianstad Plain (Kalińska-Nartiša et al. 2017a; 2017b).

Overall, the early aeolian activity inferred from the Lake Lyngsjön record (AD 1700-1720), which coincides with minimum forest cover as deduced from Buhrman's map, coincides with a regional phase of increased aeolian activity at the beginning of the 18th century as proposed by Agrell (1980) and Olsenius (2014).

Implementation of land amalgamation, which reduced the number of land parcels (Lewan 1991; Berglund et al. 1991), was initiated in 1803 at Lyngsjö village (Fig. 9) and fully implemented in 1826 (Fig. 10). The lake and the village as portrayed in 1803 indicate widespread land use in the form of arable fields. Prior to the land amalgamation in 1826, the fields were divided into smaller and enclosed parcels that counteracted wind erosion (Fig. 9). This agricultural change through land amalgamation, which would have facilitated wind erosion, was simultaneously counteracted by plantations of pine trees in the late 18th century on mainly sandy and less fertile soils regionally (Agrell 1980, 1981; Bärring et al. 2003; Ödman & Olsson 2014). The plantation of pine hampered the aeolian activity on the Kristianstad Plain until the 20th century (Agrell 1981). This increase in forest cover is also depicted on the Systematic map of Scania produced in the period of AD 1812-1820 (Fig. 11), indicating the presence of forests to the north, south-east and further south (Vittskövle area) of Lake Lyngsjön, although not in the absolute proximity of the lake. The Topographic map from 1862 indicates increased forest cover south of Lyngsjö, around Everöd village (Fig. 12). The population during the 19th century increased to 448 individuals in 1869, which is the maximum population the parish has ever had (Holmstedt 1956).

The increase in population from the 17th to the late 19th century (Fig. 6) explains the intensified land use and the subsequent increase in aeolian activity during the 18th century. Likewise, the population increase can also be partly attributed to the reduced aeolian activity by plantation of trees during the 19th century. Similar trends towards population maxima in the late 19th century and increased soil erosion have been noted in southern Scania, around the Ystad area (Berglund et al. 1991).

4.1.5 Lyng-5 (AD 1890-1930)

The onset of the 20th century is characterized by a significant increase in aeolian sand deposited in the lake, which is clearly visible by colour in unit 33 (Fig. 2). This increase suggests a period of substantial aeolian activity from the beginning of the 1900s until 1920 when the highest amount of aeolian sand within the entire succession was deposited. TOC values during this time remain low, most likely due to dilution by the massive increase in sand content (Enters et al. 2010). Simultaneously, C/N ratios steadily decrease, indicating reduced input of terrestrial organic matter together with possible introduction of artificial fertilizers (increased nitrogen supply to the lake) (Routh et al. 2004; Bragée et al. 2013). The massive input of aeolian sand probably had a negative impact on *Chara* algae (sharp decline in TIC, partially due to dilution) which had previously thrived in the lake during relatively low aeolian activity (Hammarlund et al. 2005).

This significant increase in aeolian sand deposition coincides with increased wind erosion at the beginning of the 20th century as documented for the Kristianstad Plain (Olsenius 2014). The causes of this event were

Fig. 11. Systematic map of Scania ”Skånska rekognosceringskartan” established between 1812-1820. The map displays a generally open landscape with an increase in coniferous forest cover east to southeast of Lake Lyngsjön towards Lyngby. The area near Everöd (“Efveröd”) is still devoid of forest and coniferous forests can be found further north and west, beyond the village of Östra Vram (“Ö Wram”). The original hand drawn maps are preserved at the Swedish Military Archive in Stockholm (part of the Topografiska kåren/Fältmätningskåren/Ingenjörskåren archive, available through the Swedish National Archive website). Scale of map: 1:20 000, sheet numbers VIÖ 202 and VIÖ 203.

probably mainly the previously described structural changes in agriculture, e.g. the merging of parcel units and the removal of obstacles such as fences and vegetation, which enhanced erosion of soils (Åhman 1974; Agrell 1980, 1981; Bärring et al. 2003). Furthermore, increased crop cultivation in the Lyngsjö area during the early 1900s is partially indicated by the increase in cultivated pollen such as *Avena* (oat), *Hordeum* (barley), *Secale* (rye) and *Triticum* (wheat). This can be connected to the introduction of improved machinery, which enhanced agricultural production and at the same time contributed to increased aeolian erosion (Bärring et al. 2003).

What should also be noted is the presence of trees during this time with somewhat decreased presence of pine and the plantation of *Picea* (spruce) (see Fig. 7) south of the lake around Älvasjön (a small fen) (Regnéll 1980). The presence of trees did not appear to hamper aeolian erosion during this time, although intensified land use since the 18th century might be the main reason for the noticeable amounts of aeolian sand deposited in the lake.

4.1.6 Lyng-6 (AD 1930-2013)

After the 1900s peak in aeolian activity, a phase with reduced aeolian sand deposition followed. C/N ratios continue to decrease, indicating a continuous increase in the input of nitrogen from artificial fertilizers and possibly even airborne nitrogen deposition into the lake (Routh et al. 2004; Bragée et al. 2013). It should also be noted that the absence of diagenesis in the topmost samples could have favoured the retention of nitrogen in the sediments. The TIC content increases gradually, indicating a recovery of *Chara* algae following the preceding intense aeolian sand deposition event. Furthermore, the TOC content increases while C/N ratios decrease, indicating some impact of anthropogenic nitrogen deposition which could have led to algal recovery and thus contributing to increased algal organic matter being deposited (Meyers 2003; Routh et al. 2004).

According to Regnéll (1980), pine was once more planted south of the lake between AD 1910 and 1930. The Hundred’s map from AD 1926-1934 indicates the presence of coniferous forest in the proximity, east and

Fig. 12. Topographic map (ordinance survey map) "Generalstabskartan 1827-1971", illustrating Lake Lyngsjön and village in 1862. The lake size appears to have been reduced in agreement with Regnéll (1980). The immediate lake surroundings are still without trees and an increase in coniferous forests can be seen around Everöd village ("Efveröd"). Map scale: 1:100 000, sheet number II.Ö.41 Christianstad. Map from Lantmäteriet's Historical Archive of Maps.

south of the lake (Fig. 13). The Hundred's map also shows extensive land use in the form of arable fields locally, together with coniferous forests relatively close to the lake. Additionally, air-photos from the 1940s show the area immediately west and south of the lake were covered by forest (Fig. 14), consistent with the plantation of trees 10-30 years earlier. This forest vegetation was more or less retained until 1972 as inferred from the Economic map (Fig. 15).

Following the late 19th century maximum, a steady decrease in population occurred (Fig. 6), which was most likely driven by industrialization and people moving to the cities (e.g. Berglund et al. 1991). Simultaneously with the documented reforestation in the Lyngsjö area, wind erosion appears to have increased after the 1940s in southwestern Scania and on the Kristianstad Plain (Åhman 1974; Mattson et al. 1983; Bärring et al. 2003). This indicates that the aeolian activity recorded regionally may have been reduced due to local factors such as increased forest cover and local agricultural practices, which is also inferred from the sand deposition and pollen records.

It is not until the beginning of the 21st century that a minor peak in aeolian sand deposition is recorded, with a slight impact on TOC and TIC contents, which could be due to local changes in agriculture near the lake.

4.2 Aeolian sand content and methodological considerations

The reconstructed aeolian sand accumulation rate (ASAR) represents sand grains larger than 200 µm deposited at the center of the lake. The main mode of terrestrial transportation as described by Kok et al. (2012) for grains within the range of 70-500 µm is by saltation, meaning that primarily finer particles (silt and clay) are carried in suspension by the wind (Pye & Tsoar 2009). To be able to cross a minimum distance of 100 m (the smallest radius of Lake Lyngsjön), grains larger than 200 µm have most likely been transported to the center of the lake during winter when the lake was frozen or during periods with strong winds (e.g. de Jong et al. 2006, 2007). Particularly larger grains (found in more recent samples) could also have been carried by plant debris into the lake.

The size of the lake is another important matter. The map from AD 1803 (Fig. 9), shows the first evidence of a trench connecting the northern side of the lake to the Vramsån River. The water flows from the lake to the river and the trench was dug to regulate the water level and collect drainage water from the surrounding fields (Regnéll 1980). Prior to the 1800s, there is no evidence of a trench on Buhrman's map from 1684 (Fig. 8). This is also due to the coarseness

Fig. 13. Hundred's map (economic map, "Häradsekonomiska 1859-1934") established between 1926-1934 for the Lyngsjö area. Plantation of pine can be seen close to the lake and an increase in forest cover east of the lake towards Köpinge is implied. The map indicates a noticeable extent of arable fields and pastures and a trend towards a more closed landscape in terms of forest cover compared to previous maps. Map from Lantmäteriet's Historical Archive of Maps.

Fig. 14. Air-photo from the 1940s.The photo indicates well-established coniferous forests close to the lake in an otherwise semi-open landscape. Map from Kristianstad municipality Map Archive.

Fig. 15. Economic map "Ekonomiska kartan 1935-1978" depicting Lake Lyngsjön and village in 1972. The map indicates a well -established agricultural structure, similar to today. Arable fields and pastures are still the dominant type of land use and the forest extent remains similar to the Hundred's map with a few exceptions close to the lake. Map from Lantmäteriet's Historical Archive of Maps.

of the map where finer details have not been drawn out, meaning that the trench could have been established even earlier than the 1800s. The lake as depicted in 1826 (Fig. 10) during the implementation of the land amalgamation, was according to Regnéll (1980) 45% larger compared to what he observed in the 1970s (see Fig. 15. for comparison). However, no further information on whether this was a sudden or gradual change has been found. Looking at the geochemical data and the ASAR, the only major change since 1826 would have been the 1900s increase in aeolian sand and the major decrease in TIC. Since there are no further indications supporting the hypothesis of a sudden lowering of the lake level, the lake level change would most likely have been gradual with no noteworthy impact on the recorded ASAR.

The aeolian sand content was obtained through burning of samples at 550°C. This process produces considerable amounts of ash if the majority of the macrofossils are not removed prior to ignition. The larger macrofossils were removed by hand; utilizing the difference in density between the minerogenic sand and the organic matter where the latter tends to float when water-filled samples are stirred. Samples with abundant fine-grained organic matter will generally produce more ash as compared to samples with only minerogenic material. In the reconstructed ASAR record, there are seven peaks exceeding 0.0002 g cm^{-2} $year^{-1}$(Fig. 5, Appendix 2). One sample, representing the peak recorded at AD 1840, can be disregarded due to its high clay content. The three major peaks at AD 1920, 1410 and 965, represent samples containing noticeable amounts of sand which could be clearly seen after ignition. Two of these peaks, recorded at 1920 and 1410, are both preceded by samples with increased amounts of aeolian sand, indicating prolonged intervals of wind erosion in the area. The four minor peaks occurring around AD 1170, 1700 to 1720 and at 2008, all represent samples exceeding 0.0002 g cm^{-2} $year^{-1}$. Samples with ASAR values lower than 0.0001 g cm^{-2} $year^{-1}$, have not been interpreted as evidence of aeolian activity in the area. This is due to low amounts of sand observed in most of these samples which indicates that the ash produced after ignition probably had a larger influence on the total weight.

A closer observation of the samples representing the peaks at AD 1700 (0.00026 g cm^{-2} $year^{-1}$) and AD 1720 (0.00027 g cm^{-2} $year^{-1}$), reveals very little material (mostly ash) and almost no sand. It is therefore difficult to conclude whether the 1700s was a phase with increased aeolian activity based solely on the contents of these two samples. The onset of the 1700s was as previously mentioned characterized by increased aeolian activity and dune formation on the Kristianstad Plain (Agrell 1980; Olsenius 2014; Kalińska-Nartiša 2017a, 2017b). This increases the probability that the lake area was affected by increased aeolian activity and that such an event was not registered due to limitations of the method used. However, it is also possible that the land use may not have been as intense around the lake compared to the development seen regionally.

Furthermore, rounded grains (>200 µm) of $CaCO_3$ have been found in several samples, indicating an aeolian origin and that any acid treatment to dissolve the ash would remove parts of the aeolian signal. Shell fragments, recognised as of aquatic origin, were picked out during wet sieving of the samples to reduce the impact of the non-aeolian component.

4.3 Forest cover, landscape openness and historical implications

A closer comparison of the maps in terms of forest cover extent together with written sources and the pollen data presented, helps recognizing both local and regional aeolian events recorded in the lake sediments. Considering the older aeolian peaks dated to the 10th century, 12th century and 15th century, respectively, with no available maps, the AD 965 and AD 1170 peaks are more difficult to place on a local to regional scale since written sources indicating aeolian events occurring within the given dates for the area have not been found. The landscape as inferred from the pollen data during the 10th century points towards a relatively large extent of forest cover in the region dominated by pine and birch (Fig. 7). This presence of trees as earlier mentioned coincides with relatively high C/N ratios (Fig. 5), suggesting that terrestrial organic matter could well have been derived from trees close to the lake (Kaushal & Binford 1999; Wolfe et al. 1999). The presence of nearby forests would generally hinder aeolian sand transport to the lake (Enters et al. 2010). Since there is no evidence of forest close to the lake around AD 965, the aeolian activity is more likely to be a result of increased land use with trees being present at a certain distance from the lake, similar to the 20th century landscape.

What should also be considered is that tree species such as pine and birch generally produce high amounts of pollen and can be transported longer distances, which makes it more difficult to determine their local presence (e.g. Broström et al. 2004; Eide et al. 2006). Conversely, some of the herbs and most of the cereals have a weak dispersal of pollen and are usually underrepresented in pollen diagrams, which mean that their presence in the pollen record probably reflects the immediate surroundings of the lake (e.g. Behre 1981; Lagerås 2007). On the other hand, in a more open landscape similar to the Lyngsjö area as documented by historical maps (17th century onwards), both herb and tree pollen may be transported more easily, meaning that some pollen potentially have a regional origin (Aaby 1994; Lagerås 2007). Since the pollen data are presented as percentages of the total pollen sum, some increases in e.g. tree pollen can be expected to suppress the percentages of herbs and vice versa (Bennett & Willis 2001; Lowe & Walker 2015).

The late 12th century ASAR peak occurs after a suggested regional deforestation event based on a decrease in pine pollen frequency. This decline in pine pollen (Fig. 7) during the following approximately 200 years seem to be enhanced by an increase in *Cannabis*-type pollen as a result of potential hemp retting in the lake (e.g. Lagerås 2007). Deforestation might have been a local phenomenon, which is supported by the lowered C/N ratios (Fig. 5) and reduced *Pediastrum* frequency. The aeolian activity event recorded at AD 1170 could have been a result of the loss of pine forest in the vicinity of the lake. However, it does not confirm that the increased aeolian activity was local since a decline in pine could also have occurred regionally. Apart from the changes in tree pollen frequencies, the continuous presence of *Artemisia*, *P. lanceolata* and *R. acetosa/R. acetosella* together with cultivated plants such as *Secale* and *Cannabis*-type pollen before and after the deforestation is noteworthy (Fig. 7). This implies that the 'agrarian crisis' recorded in other parts of Scania during the 14th century (e.g. Gaillard et al. 1991b; Lagerås 2007), did not have a significant impact on the area surrounding the lake. This continuation of human impact as inferred from cultural pollen further supports the occurrence of early aeolian events as a consequence of extensive land use which would have facilitated wind erosion (e.g. Åhman 1974; Bärring et al. 2003).

The 15th century increase in aeolian activity occurred during a time of slightly elevated C/N ratios (Fig. 5) and a change to a relatively open landscape as seen in a slight increase in pine abundance (Fig. 7). There are no maps to confirm the openness in the landscape. As earlier described, Agrell (1981) mentions an increase in aeolian sand drift having occurred during the 14th century as a result of deforestation in the area of Vittskövle (south of Lyngsjö village). This could well have been the onset of a regional event recorded a century later at Lake Lyngsjön due to effects of local factors. Since there is no exact date, this regional increase in sand drift could also have occurred during the late 14th century which would be closer in timing with the reconstructed aeolian activity event. A regional change with diminished extent of forests fits well as an explanation of the increase in aeolian sand deposition.

Buhrman's map (1684) further depicts the openness in the landscape. The overall crudeness of the map does not allow a detailed delineation of the forest extent although it does indicate two areas of coniferous forest situated approx. 2 km northeast and 3 km southeast of the lake and an overall open landscape regionally (the Kristianstad Plain). The scarcity of coniferous forests as indicated by the map aligns with the generally low abundance of pine (Fig. 7). Additionally the occurrence of deciduous forests, birch and beech indicated by pollen, further to the west (beyond Sönnarslöv and Östra Vram, Fig. 8) also agrees with the map. However, the 16th century war and the following 100 years of low agricultural productivity due to increased sand drift (Sallerfors 1974; Regnell 1980), together with the open landscape as portrayed on Buhrman's map, do not agree with the generally low amounts of aeolian sand deposited during the 16th and 17th century. As earlier explained, the 18th century aeolian peaks agree well with the increased aeolian activity during this time but because of the limitations of the method it cannot be confirmed solely by the aeolian sand accumulation rate (ASAR) data. Additionally, the presence of such aeolian peaks would concur with the general increase in aeolian activity documented on the Kristianstad Plain with the formation of dunes and intensified land use (Agrell 1980, 1981; Bärring et al. 2003; Olsenius 2014).

The AD 1812-1820 Systematic map of Scania (Fig. 11) and the AD 1862 Topographic map (Fig. 12) indicate the presence of forests during the 19th century. However, they do not show any forests locally (near or in the proximity of the lake), which would otherwise be expected based on the increased pine pollen frequency (Fig. 7). A small increase in coniferous trees relatively close to Lyngsjö village can be inferred from the Systematic map of Scania when compared to the forest cover on Buhrman's map (1684), indicating a slight increase in forest cover in AD 1812-1820. Deciduous forests are present further to the northwest, west and south-west of the lake towards Östra Vram and Sönnarslöv during the 1800s (Fig. 11). The decrease in aeolian sand deposition in the lake during the 19th century can be expected due to the plantation of pine regionally despite the changes related to land amalgamation which promoted wind erosion (Agrell 1980, 1981; Bärring et al. 2003; Ödman & Olsson 2014). Since there is no significant increase in pine forest cover near the lake during the 19th century, the increase in pine pollen frequency can be attributed mainly to regional changes, which is consistent with the maps.

The increased aeolian activity as recorded in the lake sediments during the 20th century is undoubtedly a consequence of increased agricultural activity locally but also regionally. Previous agricultural changes during the 19th century with merging of parcel units increased wind fetch, and subsequent mechanization during the 20th century increased the erosion of soils by wind (Åhman 1974; Agrell 1980, 1981; Bärring et al. 2003). A slight increase in the frequencies of pollen of cultivated plants between AD 1900 and 1930 to some extent affects the pine pollen frequency. It was not until after the increased deposition of aeolian sand that pine and spruce were planted in proximity of the lake in the late 1920s to 1930s (west and south) as shown by the Hundred's map (Fig. 13) and the airphoto from 1940s (Fig. 14). These two maps show a general increase in forest cover both regionally and locally.

The Economic map from 1972 (Fig. 15) indicates a continuation of similar forest coverage patterns. The 20th century maps also indicate that forest is a minor land use compared to arable fields. The ASAR peaks in the 1920s and at approx. AD 965 both occur during times of increased coniferous pollen frequencies. Since no maps are available during the 10th century, the increase in aeolian sand deposition at approx. AD 965 could have occurred due to intensified land use within Lyngsjö Parish, although coniferous forest was present locally. It should be noted that the increased aeolian activity during the 20th century was a regional event as implied by several authors (e.g. Åhman 1974; Mattson et al. 1983; Bärring et al. 2003; Olsenius 2014), which was most likely amplified by local factors near the lake, such as the extent of forest cover and intensified land use through mechanization. The elevated aeolian sand deposition recorded could also have been related to possible dune reactivation, with nearby dunes being part of the source for the aeolian sand drift during the 20th century.

5 Conclusions

The aeolian sand deposited during the last millennium had a noticeable impact on the lake development as recorded by geochemical data. The reconstructed aeolian events can be related to periods with intensified land use and alterations in forest cover on a local to regional scale. Modern aeolian sand peaks (18th century onwards) connected to documented changes of increased aeolian activity on the Kristianstad Plain together with local evidence, e.g. 19th century land amalgamation and increased forest cover close to the lake, can be used to facilitate the interpretation of 10th and 12th century aeolian sand peaks.

Elevated C/N ratios (zone Lyng-2) together with increased tree pollen (pine and birch) suggest input of terrestrial organic matter from trees relatively close to the lake. A change to lower C/N ratios (zone Lyng-3) is related to deforestation close to the lake and a shift to primarily algal production with a strong anticorrelation between TOC and TIC contents. The 18th to 19th century increase in pine pollen frequency led to elevated C/N ratios, although the increased forest cover was primarily related to changes on a regional scale based on historical maps. Declining C/N ratios during the 20th century may be attributed to modern changes in agriculture (20th century onwards) with the introduction of nitrogen fertilizers. Increased TIC content is suggested to be a result of *in situ Chara*-type algae production and terrestrial carbonates deposited in the lake. Increased aeolian sand deposition had a diluting effect on TOC and TIC together with possible increases in catchment erosion.

Aeolian activity seems to be governed primarily by changes in agriculture and secondly by forest cover. Agricultural reformation such as the 19th century land amalgamation removed wind breaking fences and vegetation, which increased the wind fetch. The 20th century agricultural mechanization added to the increase in aeolian sand transported into the lake. Increased forest cover did not hinder the deposition of aeolian sand during the 10th and 20th centuries. The late 17th century and 19th century maps indicate a change in forest cover, primarily occurring on a regional scale. The 20th century increase in forest cover as indicated by maps occurs both locally and regionally. Reconstructed changes in aeolian activity align well with historical literature and maps.

The method used to assess past aeolian activity is not suitable for detecting smaller quantities of aeolian sand. Samples with high amounts of clay need to be thoroughly sieved to avoid clumps of clay adhering to macrofossils. The 2 cm sample resolution applied appears to be sufficient for recognizing changes in regional to local aeolian activity. It is however not suitable for detecting short-lasting events that might have occurred locally on the Kristianstad Plain. For the purpose of recognizing events that coincide with documented events on a regional scale, the resolution has proven to be sufficient. Furthermore, the sediment sand record with the given dates for the aeolian peaks fits well with historical events.

Information regarding changes in wind climate was not included in this thesis, although it is possible that wind climate could have had some influence on the aeolian activity in the area.

6 Acknowledgements

I would like to thank my supervisor Dan Hammarlund for his great patience, guidance and help during the process of subsampling, especially the freeze core, and the inspirational discussions that led to this manuscript. I would also like to thank my co-supervisor Karl Ljung for the help with the initial interpretations of the geochemical data and assistance during the processing of the samples.

Thanks is also given to Åsa Wallin and Dan Hammarlund for the help during the freeze-drying of samples and with resolving the seemingly endless issues of the freeze-dryer. Leif Björkman is also thanked for the contribution of the pollen data and preliminary explanations of the land use history at the site. An additional thanks goes to Allix Baxter for the meticulous work on the Russian-core sequence, providing me with correlated cores and valuable descriptions of the lake sediments.

7 References

Aaby, B., 1994: NAP percentages as an expression of cleared areas. In B. Frenzel (ed.): *Evaluation of land surfaces cleared from forests in the Roman Iron Age and the time of migrating Germanic tribes based on regional pollen diagrams*. Paläoklimaforschung 12, 13–27. Fischer, Stuttgart, Germany.

Agrell, H., 1980: Inlandsdyner på Kristianstadslätten, östra Skåne. *In* L. Améen, K.E. Bergsten & J.O. Mattsson (eds.): Svensk Geografisk Årsbok 56, 23–37. *Sydsvenska geografiska sällskapet*.

Agrell, H., 1981: Subrecent Inland Dunes on the Kristianstad Plain, Southern Sweden. *In* L.-K. Königsson. & K. Paabo (eds.): Florilegium Florinis Dedicatum. *Striae 14*, 48–51.

Andersson Palm, L., 2000: *Folkmängden i Sveriges socknar och kommuner 1571-1997: med särskild hänsyn till perioden 1571-1751*. Books-on-demand, Göteborg. 385 pp.

Appleby, P.G., 2001: Chronostratigraphic techniques in recent sediments. *In* W.M. Last & J.P. Smol (eds.): *Tracking Environmental Change Using Lake Sediments. Volume 1: Basin Analysis, Coring, and Chronological Techniques*. Developments in paleoenvironmental research 1, 171–203. Kluwer Academic Publishers, Dordrecht, the Netherlands.

Barnekow, L., Bragée, P., Hammarlund, D. & St. Amour, N., 2008: Boreal forest dynamics in north-eastern Sweden during the last 10,000 years based on pollen analysis. *Vegetation History and Archaeobotany 17*, 687–700.

Behre, K.-E., 1981: The interpretation of anthropogenic indicators in pollen diagrams. *Pollen et Spores 23*, 225–245.

Bennett, K.D. & Willis, K.J., 2001: Pollen. *In* J.P. Smol, H.J.B. Birks & W.M. Last (eds.): *Tracking Environmental Change Using Lake Sediments. Volume 3: Terrestrial, Algal, and Siliceous Indicators*. Developments in paleoenvironmental research 3, 5–32. Kluwer Academic Publishers, Dordrecht, the Netherlands.

Berglund, B.E., Larsson, L., Lewan, N., Gunilla, E., Olsson, A. & Skansjö, S., 1991: Cultural landscape periods: patterns and processes. *In* B.E. Berglund (ed.): The Cultural Lanscape during 6000 Years in Southern Sweden. *Ecological Bulletin 41*, 427–435.

Berglund, B.E., 2007: Agrarian landscape development in northwestern Europe since the Neolithic: Cultural and climatic factors behind a regional/continental pattern. *In* A. Hornborg & C.L. Crumley (eds.): *The World System and the Earth System: Global Socioenvironmental Change and Sustainability Since the Neolithic*, 111–120. Left Coast Press.

Björkman, L., 2018: Pollenanalytisk undersökning av en lagerföljd från Lyngsjön och jordprover från röjningsrösen vid Lokal 1 och 5. Sydsvensk Arkeologi AB, Kristianstad. 108 pp.

Blaauw, M., 2010: Methods and code for 'classical' age-modelling of radiocarbon sequences. *Quaternary Geochronology 5*, 512–518.

Bradshaw, E., Rasmussen, P., Nielsen, H. & Anderson, N.J., 2005: Mid- to late-Holocene land-use change and lake development at Dallund Sø, Denmark: trends in lake primary production as reflected by algal and macrophyte remains. *The Holocene 15*, 1130–1142.

Bragée, P., Choudhary, P., Routh, J., Boyle, J.F. & Hammarlund, D., 2013: Lake ecosystem responses to catchment disturbance and airborne pollution: an 800-year perspective in southern Sweden. *Journal of Paleolimnology 50*, 545–560.

Breshears, D.D., Whicker, J.J., Zou, C.B., Field, J.P. & Allen, C.D., 2009: A conceptual framework for dryland aeolian sediment transport along the grassland-forest continuum: Effects of woody plant canopy cover and disturbance. *Geomorphology 105*, 28–38.

Brodie, C.R., Leng, M.J., Casford, J.S.L., Kendrick, C.P., Lloyd, J.M., Yongqiang, Z. & Bird, M.I., 2011: Evidence for bias in C and N concentrations and $\delta^{13}C$ composition of terrestrial and aquatic organic materials due to pre-analysis

acid preparation methods. *Chemical Geology 282*, 67–83.
Broström, A., Sugita, S. & Gaillard, M.-J., 2004: Pollen productivity estimates for the reconstruction of past vegetation cover in the cultural landscape of southern Sweden. *The Holocene 14*, 368–381.
Bärring, L., Jönsson, P., Mattsson, J.O. & Åhman, R., 2003: Wind erosion on arable land in Scania, Sweden and the relation to the wind climate: a review. *Catena 52*, 173–190.
County Administrative Board of Scania., 2016: *Bevarandeplan för Natura 2000-området Lyngsjön SE0420235*. Länsstyrelsen Skåne. 29 pp.
Dean, W.E., 1999: The carbon cycle and biogeochemical dynamics in lake sediments. *Journal of Paleolimnology 21,* 375–393.
de Jong, R., Björck, S., Björkman, L. & Clemmensen, L.B., 2006: Storminess variation during the last 6500 years as reconstructed from an ombrotrophic peat bog in Halland, southwest Sweden. *Journal of Quaternary Science 21*, 905–919.
de Jong, R., Schoning, K. & Björck, S., 2007: Increased aeolian activity during humidity shifts as recorded in a raised bog in south-west Sweden during the past 1700 years. *Climate of the Past 3*, 411–422.
Eide, W., Birks, H.H., Bigelow, N.H., Peglar, S.M. & Birks, H.J.B., 2006: Holocene forest development along the Setesdal valley, southern Norway, reconstructed from macrofossil and pollen evidence. *Vegetation History and Archaeobotany 15*, 65–85.
Enters, D., Lücke, A. & Zolitschka, B., 2006: Effects of land-use change on deposition and composition of organic matter in Frickenhauser See, northern Bavaria, Germany. *Science of the Total Environment 369*, 178–187.
Enters, D., Dörfler, W. & Zolitschka, B., 2008: Historical soil erosion and land-use change during the last two millennia recorded in lake sediments of Frickenhauser See, northern Bavaria, central Germany. *The Holocene 18*, 243–254.
Enters, D., Kirilova, E., Lotter, A.F., Lücke, A., Parplies, J., Jahns, S., Kuhn, G. & Zolitschka, B., 2010: Climate change and human impact at Sacrower See (NE Germany) during the past 13,000 years: a geochemical record. *Journal of Paleolimnology 43*, 719–737.
Friman, B. & Hyll, N., 2015: *E22 sträckan Sätaröd-Vä: Skåne, Kristianstads kommun, Linderöd, Västra Vram och Vä socken*. National Historical Museums and Archeological Assignments, Rapport 30. 93 pp.
Gaillard, M.-J. & Berglund, B.E., 1988: Land-use History during the Last 2700 Years in the area of Bjäresjö, Southern Sweden. *In* H.H. Birks, H.J.B. Birks, P.E. Kaland & D. Moe (eds.): *The Cultural Landscape: Past, Present and Future*, 409–428. Cambridge University Press, Cambridge, United Kingdom.
Gaillard, M.-J., Dearing, J.A., El-Daoushy, F., Enell, M. & Håkansson, H., 1991a: A late Holocene record of land-use history, soil erosion, lake trophy and lake-level fluctuations at Bjäresjösjön (South Sweden). *Journal of Paleolimnology 6*, 51–81.
Gaillard, M.-J., Dearing, J.A., El-Daoushy, F., Enell, M. & Håkansson, H., 1991b: A multidisciplinary study of the lake Bjäresjösjön (S Sweden): land-use history, soil erosion, lake trophy and lake-level fluctuations during the last 3000 years. *Hydrobiologia 214*, 107–114.
Hammarlund, D., Björck, S., Buchardt, B. & Thomsen, C.T., 2005: Limnic responses to increased effective humidity during the 8200 cal. yr BP cooling event in southern Sweden. *Journal of Paleolimnology 34,* 471–480.
Holmstedt, F., 1956: *Lyngsjö: kyrkan och socknen genom tiderna*. Lyngsjö församling, Gärds Köpinge. 98 pp.
Juggins, S., 2007: *C2: Software for ecological and palaeoecological data analysis and visualization: User guide Version 1.5*. Newcastle University, Newcastle upon Tyne, United Kingdom. 73 pp.
Kalińska-Nartiša, E., Alexanderson, H. & Nartišs, M., 2017a: Luminescence dating of aeolian-coastal events on the Kristianstad plain, SE Sweden. *The Holocene 27*, 85–97.
Kalińska-Nartiša, E., Alexanderson, H., Nartišs, M., Stevic, M. & Kaiser, K., 2017b: Sedimentary features reveal transport paths for Holocene sediments on the Kristianstad coastal plain, SE Sweden. *GFF 139*, 147–161.
Kaushal, S. & Binford, M.W., 1999: Relationship between C:N ratios of lake sediments, organic matter sources, and historical deforestation in Lake Pleasant, Massachusetts, USA. *Journal of Paleolimnology 22*, 439–442.
Kok, J.F., Parteli, E.J.R., Michaels, T.I. & Bou Karam, D., 2012: *The physics of wind-blown sand and dust*. Reports on Progress in Physics 75. 119 pp.
Köster, D., Pienitz, R., Wolfe, B.B., Barry, S., Foster, D.R. & Dixit, S.S., 2005: Paleolimnological assessment of human-induced impacts on Walden Pond (Massachusetts, USA) using diatoms and stable isotopes. *Aquatic Ecosystem Health and Management 8*, 117–131.
Lagerås, P., 1996: Long-term history of land-use and vegetation at Femtingagölen: a small lake in the

Småland Uplands, southern Sweden. *Vegetation History and Archaeobotany 5*, 215–228.
Lagerås, P., 2004: Landskapet längs E22:an: Naturgeografisk zonindelning av vägens närområde genom Skåne och Blekinge. National Heritage Board, UV Syd Rapport 17. 7 pp.
Lagerås, P., 2007: *The Ecology of Expansion and Abandonment: Medieval and Post-Medieval Land-use and Settlement Dynamics in a Landscape Perspective*. National Heritage Board, Stockholm. 256 pp.
Lewan, N., 1991: The age of enclosure and improvement in agriculture. *In* B.E. Berglund (ed.): The Cultural Lanscape during 6000 Years in Southern Sweden. *Ecological Bulletin 41*, 380–387.
Li, X.-Y., Liu, L.-Y. & Wang, J.-H., 2004: Wind tunnel simulation of aeolian sandy soil erodibility under human disturbance. *Geomorphology 59*, 3–11.
Li, L., Yu, Z., Moeller, R.E. & Bebout, G.E., 2008: Complex trajectories of aquatic and terrestrial ecosystem shifts caused by multiple human-induced environmental stresses. *Geochimica et Cosmochimica Acta 72*, 4338–4351.
Lidmar-Bergström, K., Mattsson, J.O., Rapp, A. & Åkerman, J., 1983: *Guider för naturgeografiska exkursioner genom områden i Skåne med vinderosion respektive preglacialt landskap*. Lund University, Department of Human Geography, Rapporter och notiser 54, 11 pp.
Linné, C., 1751: *Carl Linnæi, Archiat. Reg. Et. Med. Prof. Upsal. Skånska resa, på höga öfwerhetens befallning förrättad år 1749. Med rön och anmärkningar uti oeconomien, naturalier, antiquiteter, seder, lefnads-sätt. Med tillhörige figurer. Med kongl. maj:ts allernådigste privilegio*. Lars Salvii, Stockholm. 468 pp.
Lowe, J. & Walker, M., 2015: *Reconstructing Quaternary Environments*. Routledge, London. 538 pp.
Mattsson, J.O., Rapp, A. & Åhman, R., 1978: Vinderosion i Skåne våren 1978. In K.E. Bergsten, L. Améen & J.O. Mattson (eds.): Svensk Geografisk Årsbok 54, 103–110. *Sydsvenska geografiska sällskapet*.
Mattsson, J.O., Nihlén, T. & Olesen, F., 1983: Vindens skadegörelse på åkermark i Skåne och Danmark. In B. Lenntorp, A. Rapp & G. Törnqvist (eds.): Svensk Geografisk Årsbok 59, 34–59. *Sydsvenska geografiska sällskapet*.
Meyers, P.A. & Lallier-Vergès, E., 1999: Lacustrine sedimentary organic matter records of Late Quaternary paleoclimates. *Journal of Paleolimnology 21*, 345–372.
Meyers, P.A. & Teranes, J.L., 2001: Sediment organic matter. *In* W.M. Last & J.P. Smol (eds.): *Tracking Environmental Change Using Lake Sediments. Volume 2: Physical and Geochemical Methods*. Developments in paleoenvironmental research 2, 239–262. Kluwer Academic Publishers, Dordrecht, the Netherlands.
Meyers, P.A., 2003: Applications of organic geochemistry to paleolimnological reconstructions: a summary of examples from the Laurentian Great Lakes. *Organic Geochemistry 34*, 261–289.
Nõges, P., Tuvikene, L., Feldmann, T., Tõnno, I., Künnap, H., Luup, H., Salujõe, J. & Nõges, T., 2003: The role of charophytes in increasing water transparency: a case study of two shallow lakes in Estonia. *Hydrobiologia 506–509*, 567–573.
Olsenius, B., 2014: *Vinderosion, sanddrift och markanvändning på Kristianstadsslätten*. Undergraduate Thesis 409, Lund University, Department of Geology, Lund. 38 pp.
Pye, K. & Tsoar, H., 2009: *Aeolian sand and sand dunes*. Springer, Berlin. 458 pp.
Rasmussen, P. & Anderson, N.J., 2005: Natural and anthropogenic forcing of aquatic macrophyte development in a shallow Danish lake during the last 7000 years. *Journal of Biogeography 32*, 1993–2005.
Rasmussen, P. & Olsen, J., 2009: Soil erosion and land-use change during the last six millennia recorded in lake sediments of Gudme Sø, Fyn, Denmark. *Geological Survey of Denmark and Greenland Bulletin 17*, 37–40.
Ravi, S., Breshears, D.D., Huxman, T.E. & D'Odorico, P., 2010: Land degradation in drylands: Interactions among hydrologic-aeolian erosion and vegetation dynamics. *Geomorphology 116*, 236–245.
R Development Core Team., 2016: *R: A language and environment for statistical computing*. R Foundation for Statistical Computing, Vienna, Austria.
Regnéll, G., 1980: *Naturvårdsundersökning kring Lyngsjön i Kristianstads län: inventering och förslag till avgränsning och riktlinjer för ett framtida naturreservat*. Meddelanden från Växtekologiska institutionen Lunds universitet 42, Lund. 53 pp.
Reimer, P.J., Bard, E., Bayliss, A., Beck, J.W., Blackwell, P.G., Bronk Ramsey, C., Buck, C.E., Cheng, H., Edwards, R.L., Friedrich, M., Grootes, P.M., Guilderson, T.P., Haflidason, H., Hajdas, I., Hatté, C., Heaton, T.J., Hoffman, D.L., Hogg, A.G., Hughen, K.A., Kaiser, K.F., Kromer, B., Manning, S.W., Niu, M., Reimer, R.W., Richards, D.A., Scott, E.M., Southon, J.R., Staff, R.A., Turney, C.S.M., van der Plicht, J., 2013: IntCal13 and Marine13 Radio-

carbon Age Calibration Curves 0-50,000 Years cal BP. *Radiocarbon 55*, 1869–1887.
Routh, J., Meyers, P.A., Gustafsson, Ö., Baskaran, M., Hallberg, R. & Schöldström, A., 2004: Sedimentary geochemical record of human-induced environmental changes in the Lake Brunnsviken watershed, Sweden. *Limnology and Oceanography 49*, 1560–1569.
Sallerfors, S.-E., 1974: *Gärds härad under dansk tid: bebyggelse och befolkning*. Licentiate Thesis, Lund University, Department of History, Lund. 225 pp.
Swedish Environmental Protection Agency., 2000: *Registerblad*. Naturvårdsverket. 3 pp.
Verardo, D.J., Froelich, P.N. & McIntyre, A., 1990: Determination of organic carbon and nitrogen in marine sediments using the Carlo Erba NA-1500 Analyzer. *Deep-Sea Research 37*, 157–165.
Weibull, M., 1891: Anders Tidströms resa i Halland, Skåne och Blekinge år 1756: Med rön och anmärkningar uti oeconomien, naturalier, antiqviteter, seder, lefnads-sätt. De Skånska landskapens historiska och arkeologiska förening, Lund. 83 pp.
Wesenbeeg-Lund, C., 1901: Studier over søkalk, bønnemalm og søgytje i danske indsøer. *Bulletin of the Geological Society of Denmark 2*, 7–78.
Wolfe, B.B., Edwards, T.W.D. & Aravena, R., 1999: Changes in carbon and nitrogen cycling during tree-line retreat recorded in the isotopic content of lacustrine organic matter, western Taimyr Peninsula, Russia. *The Holocene 9*, 215–222.
Yamamuro, M. & Kayanne, H., 1995: Rapid direct determination of organic carbon and nitrogen in carbonate-bearing sediments with a Yanaco MT-5 CHN analyzer. *Limnology and Oceanography 40*, 1001–1005.
Åhman, R., 1974: Vinderosion i Sydskåne. *In* K.E. Bergsten (ed.): Svensk Geografisk Årsbok 50, 232–240. *Sydsvenska geografiska sällskapet*.
Ödman, A.M. & Olsson, P.A., 2014: Conservation of Sandy Calcareous Grassland: What Can Be Learned from the Land Use History?. *PLOS ONE 9*, 1–10.

Appendix 1. ^{210}Pb chronology of Lake Lyngsjön freeze core sequence. The ^{210}Pb dates were used to construct the upper part of the age-depth model (Fig. 4A and B, displayed in green).

Depth	**Dry mass**	**Chronology**			**Sedimentation Rate**		
		Date	**Age**				
cm	g cm^{-2}	AD	yr	±	g cm^{-2} yr^{-1}	cm yr^{-1}	± %
0	0	2013	0				
1.5	0.0826	2010	3	2	0.0237	0.463	10.3
4	0.2042	2005	8	2	0.0304	0.659	9.8
6	0.29	2002	11	2	0.0303	0.684	11.4
10	0.4698	1995	18	2	0.0229	0.518	11.2
14	0.6438	1989	24	2	0.0287	0.648	15
18	0.8246	1982	31	3	0.0231	0.508	17.6
20	0.9165	1978	35	4	0.0235	0.503	18.7
22	1.012	1973	40	4	0.0205	0.435	21.3
24	1.1045	1969	44	5	0.0246	0.539	24.4
26	1.1945	1965	48	6	0.0228	0.475	25.9
28	1.2963	1956	57	7	0.0106	0.2	28.3
30	1.4065	1945	68	8	0.0083	0.148	31.1
32	1.5194	1929	84	9	0.0065	0.1	38.6
34	1.6672	1905	108	19	0.0062	0.083	44.6

Appendix 2. Detailed information of samples from the freeze core and Russian-core sequence from Lake Lyngsjön. Sample numbers indicate samples from the freeze core sequence (F1-F39) and the Russian-core sequence (L133-L25). Samples L24-L1 represent deeper samples outside the scope of this project and were only used for radiocarbon dating; to establish an age-depth model for the combined sediment sequence. Depth interval indicates the sample resolution. IR (ignition residue) weight represents the sample weight after ignition at 550°C, scale precision of four decimals. The mineral matter concentration (g cm^{-3}) was calculated by dividing the IR weight with the sample volume. Sedimentation rate (SR, cm $year^{-1}$) were obtained from the age-depth model (Fig.4). The aeolian sand accumulation rate (ASAR) represent: SR (cm $year^{-1}$) x Mineral matter conc. (g cm^{-3}).

Sample no.	**Depth interval (cm)**	**Sample volume (cm^3)**	**IR weight (g)**	**Mineral matter conc. (g cm^{-3})**	**Sedimentation rate (cm $year^{-1}$)**	**ASAR (g cm^{-2} $year^{-1}$)**
F1	500-503	99	0.0097	0.00010	1	0.00010
F2	503-505	74	0.0386	0.00052	0.5	0.00026
F3	505-507	81	0.0351	0.00043	0.5	0.00022
F4	507-509	76	0.0102	0.00014	0.5	0.00007
F5	509-511	79	0.0081	0.00010	0.5	0.00005
F6	511-513	90	0.0129	0.00014	0.4	0.00006
F7	513-515	87	0.0194	0.00022	0.5	0.00011
F8	515-517	79	0.0151	0.00019	0.4	0.00008
F9	517-519	81	0.0095	0.00012	0.4	0.00005
F10	519-521	80	0.0134	0.00017	0.4	0.00007
F11	521-523	78	0.0226	0.00029	0.3	0.00010
F12	523-525	82	0.0166	0.00020	0.3	0.00007
F13	525-527	86	0.0171	0.00020	0.3	0.00007
F14	527-529	69	0.0127	0.00018	0.3	0.00006
F15	529-531	70	0.0155	0.00022	0.3	0.00006
F16	531-533	82	0.0567	0.00069	0.3	0.00020
F17	533-535	92	0.1264	0.00137	0.3	0.00039
F18	535-537	89	0.2591	0.00293	0.3	0.00084
F19	537-539	87	0.2201	0.00254	0.3	0.00063
F20	539-541	78	0.1085	0.00139	0.3	0.00040
F21	541-543	80	0.1389	0.00174	0.3	0.00043
F22	543-545	86	0.1050	0.00121	0.3	0.00030
F23	545-547	84	0.0645	0.00077	0.2	0.00017
F24	547-549	84	0.0230	0.00027	0.3	0.00007
F25	549-551	80	0.0184	0.00023	0.3	0.00006
F26	551-553	87	0.0349	0.00040	0.2	0.00009
F27	553-555	89	0.0417	0.00047	0.2	0.00010
F28	555-557	79	0.1132	0.00143	0.2	0.00032
F29	557-559	80	0.0369	0.00046	0.2	0.00010
F30	559-561	83	0.0335	0.00040	0.2	0.00009
F31	561-563	99	0.0364	0.00037	0.2	0.00008
F32	563-565	96	0.0372	0.00039	0.2	0.00009
F33	565-567	99	0.0276	0.00028	0.2	0.00006
F34	567-569	93	0.0460	0.00049	0.2	0.00010
F35	569-571	98	0.0304	0.00031	0.2	0.00007
F36	571-773	89	0.0329	0.00037	0.2	0.00008
F37	573-575	84	0.0503	0.00060	0.2	0.00012
F38	575-577	74	0.0382	0.00052	0.2	0.00011
F39	577-579	79	0.0258	0.00033	0.2	0.00007
L133	581-579	10	0.0021	0.00021	0.2	0.00005
L132	583-581	6	0.0072	0.00120	0.2	0.00027
L131	585-583	9	0.0060	0.00067	0.2	0.00013
L130	587-585	5	0.0058	0.00116	0.2	0.00026
L129	589-587	13	0.0084	0.00065	0.2	0.00014
L128	591-589	39	0.0085	0.00022	0.2	0.00004
L127	593-591	55	0.0123	0.00022	0.2	0.00005
L126	595-593	43	0.0176	0.00041	0.2	0.00009

Sample no.	Depth interval (cm)	Sample volume (cm^3)	IR weight (g)	Mineral matter conc. ($g\ cm^{-3}$)	Sedimentation rate ($cm\ year^{-1}$)	ASAR ($g\ cm^{-2}\ year^{-1}$)
L125	597-595	33	0.0120	0.00036	0.2	0.00008
L124	599-597	33	0.0089	0.00027	0.2	0.00006
L123	601-599	35	0.0064	0.00018	0.2	0.00004
L122	603-601	32	0.0086	0.00027	0.2	0.00006
L121	605-603	33	0.0077	0.00023	0.2	0.00005
L120	607-605	35	0.0146	0.00042	0.2	0.00009
L119	609-607	31	0.0162	0.00052	0.2	0.00012
L118	611-609	23	0.0138	0.00060	0.3	0.00015
L117	613-611	8	0.0031	0.00039	0.2	0.00009
L116	615-613	45	0.0092	0.00020	0.2	0.00005
L115	617-615	39	0.0167	0.00043	0.3	0.00011
L114	619-617	53	0.0194	0.00037	0.2	0.00008
L113	621-619	70	0.0284	0.00041	0.3	0.00010
L112	623-621	70	0.0445	0.00064	0.3	0.00016
L111	625-623	83	0.0193	0.00023	0.2	0.00005
L110	627-625	67	0.0140	0.00021	0.3	0.00005
L109	629-627	77	0.0139	0.00018	0.3	0.00005
L108	631-629	81	0.0111	0.00014	0.3	0.00003
L107	634-631	27	0.0052	0.00019	0.3	0.00005
L106	636-634	44	0.0081	0.00018	0.3	0.00005
L105	638-636	37	0.0048	0.00013	0.3	0.00003
L104	640-638	35	0.0053	0.00015	0.3	0.00004
L103	642-640	36	0.0043	0.00012	0.3	0.00003
L102	644-642	33	0.0077	0.00023	0.3	0.00006
L101	646-644	36	0.0056	0.00016	0.3	0.00004
L100	648-646	35	0.0096	0.00027	0.3	0.00008
L99	650-648	39	0.0091	0.00023	0.3	0.00006
L98	652-650	33	0.0061	0.00018	0.3	0.00005
L97	654-652	35	0.0169	0.00048	0.3	0.00014
L96	656-654	29	0.0469	0.00162	0.3	0.00040
L95	658-656	31	0.0370	0.00119	0.3	0.00030
L94	660-658	37	0.0206	0.00056	0.3	0.00014
L93	662-660	33	0.0106	0.00032	0.3	0.00008
L92	664-662	39	0.0042	0.00011	0.3	0.00003
L91	666-664	57	0.0112	0.00020	0.3	0.00005
L90	668-666	50	0.0126	0.00025	0.3	0.00006
L89	670-668	38	0.0149	0.00039	0.2	0.00009
L88	672-670	53	0.0177	0.00033	0.3	0.00008
L87	674-672	65	0.0168	0.00026	0.3	0.00006
L86	676-674	35	0.0122	0.00035	0.2	0.00008
L85	678-676	55	0.0157	0.00029	0.2	0.00006
L84	680- 678	29	0.0104	0.00036	0.2	0.00008
L83	682-680	48	0.0222	0.00046	0.3	0.00012
L82	683.5-682	49	0.0105	0.00021	0.2	0.00005
L81	685.5-683.5	27	0.0022	0.00008	0.2	0.00002
L80	687.5-685.5	35	0.0203	0.00058	0.2	0.00013
L79	689.5-687.5	35	0.0163	0.00047	0.2	0.00010
L78	690.5-689.5	18	0.0112	0.00062	0.2	0.00012
L77	692.5-690.5	37	0.0073	0.00020	0.2	0.00004
L76	693.5-692.5	18	0.0037	0.00021	0.2	0.00004

Sample no.	Depth interval (cm)	Sample volume (cm^3)	IR weight (g)	Mineral matter conc. ($g\ cm^{-3}$)	Sedimentation rate ($cm\ year^{-1}$)	ASAR ($g\ cm^{-2}\ year^{-1}$)
L75	695-693.5	28	0.0079	0.00028	0.2	0.00006
L74	697-695	36	0.0099	0.00028	0.2	0.00006
L73	698.5-697	13	0.0077	0.00059	0.2	0.00012
L72	700-698.5	45	0.0102	0.00023	0.2	0.00005
L71	702-700	37	0.0128	0.00035	0.2	0.00007
L70	704-702	40	0.0135	0.00034	0.2	0.00007
L69	706-704	61	0.0330	0.00054	0.2	0.00011
L68	708-706	65	0.0337	0.00052	0.2	0.00010
L67	710-708	65	0.1007	0.00155	0.2	0.00028
L66	712-710	68	0.0351	0.00052	0.2	0.00010
L65	714-712	72	0.0316	0.00044	0.2	0.00008
L64	716-714	63	0.0334	0.00053	0.2	0.00011
L63	718-716	60	0.0269	0.00045	0.2	0.00008
L62	720-718	40	0.0073	0.00018	0.2	0.00003
L61	722-720	32	0.0145	0.00045	0.2	0.00008
L60	724-722	33	0.0166	0.00050	0.2	0.00009
L59	726-724	35	0.0259	0.00074	0.2	0.00013
L58	728-726	39	0.0264	0.00068	0.2	0.00012
L57	730-728	41	0.0208	0.00051	0.2	0.00008
L56	732-730	40	0.0158	0.00040	0.2	0.00007
L55	734-732	35	0.0145	0.00041	0.2	0.00007
L54	736-734	43	0.0297	0.00069	0.2	0.00012
L53	738-736	33	0.0236	0.00072	0.2	0.00012
L52	740-738	8	0.0084	0.00105	0.2	0.00019
L51	742-740	13	0.0030	0.00023	0.2	0.00004
L50	744-742	10	0.0044	0.00044	0.2	0.00007
L49	746-744	9	0.0227	0.00252	0.2	0.00042
L48	748-746	11	0.0066	0.00060	0.2	0.00010
L47	750-748	6	0.0069	0.00115	0.2	0.00018
L46	752-750	28	0.0268	0.00096	0.2	0.00016
L45	754-752	24	0.0051	0.00021	0.2	0.00003
L44	756-754	33	0.0199	0.00060	0.2	0.00009
L43	758-756	36	0.0250	0.00069	0.2	0.00011
L42	760-758	37	0.0163	0.00044	0.2	0.00007
L41	762-760	28	0.0171	0.00061	0.2	0.00009
L40	764-762	12	0.0146	0.00122	0.2	0.00019
L39	766-764	12	0.0061	0.00051	0.1	0.00007
L38	768-766	13	0.0075	0.00058	0.2	0.00009
L37	770-768	13	0.0075	0.00058	0.1	0.00008
L36	772-770	13	0.0069	0.00053	0.1	0.00008
L35	774-772	9	0.0013	0.00014	0.1	0.00002
L34	775.5-774	9	0.0007	0.00008	0.1	0.00001
L33	777.5-775.5	15	0.0032	0.00021	0.1	0.00003
L32	779.5-777.5	9	0.0007	0.00008	0.1	0.00001
L31	781.5-779.5	13	0	0	0.1	0
L30	783.5-781.5	9	0.0012	0.00013	0.1	0.00002
L29	785.5-783.5	11	0.0005	0.00005	0.1	0.00001
L28	787.5-785.5	11	0.0020	0.00018	0.1	0.00002
L27	789.5-787.5	9	0.0006	0.00007	0.1	0.00001
L26	791.5-789.5	13	0.0010	0.00008	0.1	0.00001
L25	793.5-791.5	13	0.0005	0.00004	0.1	0.00001

Tidigare skrifter i serien ”Examensarbeten i Geologi vid Lunds universitet”:

498. Bergcrantz, Jacob, 2017: Ett fönster till Kattegatts förflutna genom analys av bottenlevande foraminiferer. (15 hp)
499. O'Hare, Paschal, 2017: Multiradionuclide evidence for an extreme solar proton event around 2610 BP. (45 hp)
500. Goodship, Alastair, 2017: Dynamics of a retreating ice sheet: A LiDAR study in Värmland, SW Sweden. (45 hp)
501. Lindvall, Alma, 2017: Hur snabbt påver-kas och nollställs luminiscenssignaler under naturliga ljusförhållanden? (15 hp)
502. Sköld, Carl, 2017: Analys av stabila isotoper med beräkning av blandningsförhållande i ett grundvattenmagasin i Älvkarleby-Skutskär. (15 hp)
503. Sällström, Oskar, 2017: Tolkning av geofysiska mätningar i hammarborrhål på södra Gotland. (15 hp)
504. Ahrenstedt, Viktor, 2017: Depositional history of the Neoproterozoic Visingsö Group, south-central Sweden. (15 hp)
505. Schou, Dagmar Juul, 2017: Geometry and faulting history of the Long Spur fault zone, Castle Hill Basin, New Zealand. (15 hp)
506. Andersson, Setina, 2017: Skalbärande marina organismer och petrografi av tidigcampanska sediment i Kristianstadsbassängen – implikationer på paleomiljö. (15 hp)
507. Kempengren, Henrik, 2017: Föroreningsspridning från kustnära deponi: Applicering av Landsim 2.5 för modellering av lakvattentransport till Östersjön. (15 hp)
508. Ekborg, Charlotte, 2017: En studie på samband mellan jordmekaniska egen-skaper och hydrodynamiska processer när erosion påverkar släntstabiliteten vid ökad nederbörd. (15 hp)
509. Silvén, Björn, 2017: LiDARstudie av glaciala landformer sydväst om Söderåsen, Skåne, Sverige. (15 hp)
510. Rönning, Lydia, 2017: Ceratopsida dinosauriers migrationsmönster under krit-tiden baserat på paleobiogeografi och fylogeni. (15 hp)
511. Engleson, Kristina, 2017: Miljökonsekvensbeskrivning Revinge brunnsfält. (15 hp)
512. Ingered, Mimmi, 2017: U-Pb datering av zirkon från migmatitisk gnejs i Delsjöområdet, Idefjordenterrängen. (15 hp)
513. Kervall, Hanna, 2017: EGS - framtidens geotermiska system. (15 hp)
514. Walheim, Karin, 2017: Kvartsmineralogins betydelse för en lyckad luminiscensdatering. (15 hp)
515. Aldenius, Erik, 2017: Lunds Geotermisystem, en utvärdering av 30 års drift. (15 hp)
516. Aulin, Linda, 2017: Constraining the duration of eruptions of the Rangitoto volcano, New Zealand, using paleomagnetism. (15 hp)
517. Hydén, Christina Engberg, 2017: Drumlinerna i Löberöd - Spår efter flera isrörelseriktningar i mellersta Skåne. (15 hp)
518. Svantesson, Fredrik, 2017: Metodik för kartläggning och klassificering av erosion och släntstabilitet i vattendrag. (45 hp)
519. Stjern, Rebecka, 2017: Hur påverkas luminiscenssignaler från kvarts under laboratorieförhållanden? (15 hp)
520. Karlstedt, Filippa, 2017: P-T estimation of the metamorphism of gabbro to garnet amphibolite at Herrestad, Eastern Seg-ment of the Sveconorwegian orogen. (45 hp)
521. Önnervik, Oscar, 2017: Ooider som naturliga arkiv för förändringar i havens geokemi och jordens klimat. (15 hp)
522. Nilsson, Hanna, 2017: Kartläggning av sand och naturgrus med hjälp av resistivitetsmätning på Själland, Danmark. (15 hp)
523. Christensson, Lisa, 2017: Geofysisk undersökning av grundvattenskydd för planerad reservvattentäkt i Mjölkalånga, Hässleholms kommun. (15 hp)
524. Stamsnijder, Joaen, 2017: New geochronological constraints on the Klipriviersberg Group: defining a new Neoarchean large igneous province on the Kaapvaal Craton, South Africa. (45 hp)
525. Becker Jensen, Amanda, 2017: Den eo-cena Furformationen i Danmark: excep-tionella bevaringstillstånd har bidragit till att djurs mjukdelar fossiliserats.(15 hp)
526. Radomski, Jan, 2018: Carbonate sedimentology and carbon isotope stratigraphy of the Tallbacken-1 core, early Wenlock Slite Group, Gotland, Sweden. (45 hp)
527. Pettersson, Johan, 2018: Ultrastructure and biomolecular composition of sea tur-tle epidermal remains from the Campa-nian (Upper Cretaceous) North Sulphur River of Texas. (45 hp)
528. Jansson, Robin, 2018: Multidisciplinary perspective on a natural attenuation zone in a PCE contaminated aquifer. (45 hp)
529. Larsson, Alfred, 2018: Rb-Sr sphalerite data and implications for the source and timing of Pb-Zn deposits at the Ca-ledonian margin in Sweden. (45 hp)
530. Balija, Fisnik, 2018: Stratigraphy and pyrite geochemistry of the Lower–Upper Ordovician in the Lerhamn and Fågelsång -3 drill cores, Scania, Sweden. (45 hp)
531. Höglund, Nikolas, 2018: Groundwater chemistry evaluation and a GIS-based approach for determining groundwater potential in

Mörbylånga, Sweden. (45 hp)

532. Haag, Vendela, 2018: Studie av mikrostrukturer i karbonatslagkäglor från nedslagsstrukturen Charlevoix, Kanada. (15 hp)
533. Hebrard, Benoit, 2018: Antropocen – vad, när och hur? (15 hp)
534. Jancsak, Nathalie, 2018: Åtgärder mot kusterosion i Skåne, samt en fallstudie av erosionsskydden i Löderup, Ystad kom-mun. (15 hp)
535. Zachén, Gabriel, 2018: Mesosideriter – redogörelse av bildningsprocesser samt SEM-analys av Vaca Muertameteoriten. (15 hp)
536. Fägersten, Andreas, 2018: Lateral variability in the quantification of calcareous nannofossils in the Upper Triassic, Austria. (15 hp)
537. Hjertman, Anna, 2018: Förutsättningar för djupinfiltration av ytvatten från Ivösjön till Kristianstadbassängen. (15 hp)
538. Lagerstam, Clarence, 2018: Varför svalde svanödlor (Reptilia, Plesiosauria) stenar? (15 hp)
539. Pilser, Hannes, 2018: Mg/Ca i bottenlevande foraminiferer, särskilt med avseende på temperaturer nära 0°C. (15 hp)
540. Christiansen, Emma, 2018: Mikroplast på och i havsbotten - Utbredningen av mikroplaster i marina bottensediment och dess påverkan på marina miljöer. (15 hp)
541. Staahlnacke, Simon, 2018: En sammanställning av norra Skånes prekambriska berggrund. (15 hp)
542. Martell, Josefin, 2018: Shock metamor-phic features in zircon grains from the Mien impact structure - clues to condi-tions during impact. (45 hp)
543. Chitindingu, Tawonga, 2018: Petrological characterization of the Cambrian sandstone reservoirs in the Baltic Basin, Sweden. (45 hp)
544. Chonewicz, Julia, 2018: Dimensionerande vattenförbrukning av grundvatten samt alternativa vattenkvaliteter. (15 hp)
545. Adeen, Lina, 2018: Hur lämpliga är de geofysiska metoderna resistivitet och IP för kartläggning av PFOS? (15 hp)
546. Nilsson Brunlid, Anette, 2018: Impact of southern Baltic sea-level changes on landscape development in the Verkeån River valley at Haväng, southern Sweden, dur-ing the early and mid Holocene. (45 hp)
547. Perälä, Jesper, 2018: Dynamic Recrystallization in the Sveconorwegian Frontal Wedge, Småland, southern Sweden. (45 hp)
548. Artursson, Christopher, 2018: Stratigra-phy, sedimentology and geophysical as-sessment of the early Silurian Halla and Klinteberg formations, Altajme core, Got-land, Sweden. (45 hp)
549. Kempengren, Henrik, 2018: Att välja den mest hållbara efterbehandlingsmetoden vid sanering: Applicering av beslutsstödsverktyget SAMLA. (45 hp)
550. Andreasson, Dagnija, 2018: Assessment of using liquidity index for the approxi-mation of undrained shear strength of clay tills in Scania. (45 hp)
551. Ahrenstedt, Viktor, 2018: The Neoproterozoic Visingsö Group of southern Sweden: Lithology, sequence stratigraphy and provenance of the Middle Formation. (45 hp)
552. Berglund, Marie, 2018: Basaltkuppen - ett spel om mineralogi och petrologi. (15 hp)
553. Hernnäs, Tove, 2018: Garnet amphibolite in the internal Eastern Segment, Sveconorwegian Province: monitors of metamorphic recrystallization at high temperature and pressure during Sveconorwegian orogeny. (45 hp)
554. Halling, Jenny, 2019: Characterization of black rust in reinforced concrete struc-tures: analyses of field samples from southern Sweden. (45 hp)
555. Stevic, Marijana, 2019: Stratigraphy and dating of a lake sediment record from Lyngsjön, eastern Scania - human impact and aeolian sand deposition during the last millennium. (45 hp)

LUNDS UNIVERSITET

Geologiska institutionen
Lunds universitet
Sölvegatan 12, 223 62 Lund